

Glacial to postglacial submarine landform assemblages in fiords of northeastern Baffin Island

Etienne Brouard ^{*}, Patrick Lajeunesse

Centre d'études nordiques, Département de géographie, Université Laval, Québec, Québec, Canada



ARTICLE INFO

Article history:

Received 3 October 2018

Received in revised form 7 January 2019

Accepted 8 January 2019

Available online 15 January 2019

Keywords:

Fiords

Arctic Canada

Laurentide Ice Sheet dynamics

Glacial geomorphology

ABSTRACT

Fiord morphology plays a fundamental role in glacier flow dynamics and on ice-margin stability. As most of the present-day margins of the Greenland Ice Sheet lies in fiords, there is a need for understanding short- and long-term glacial dynamics in fiord settings. We investigate ice-sheet retreat patterns in previously glaciated submarine terrain of northeastern Baffin Island fiords to provide analogues for modern and future ice-sheet response to climate change and sea-level rise. Geomorphological maps constructed from the interpretation of swath bathymetry imagery in fiords of northeastern Baffin Island reveal a wide range of glacial to postglacial landforms that allow the reconstruction of past ice-sheet retreat dynamics. Ice-flow landforms such as mega-scale glacial lineations, crag-and-tails, and meltwater channels reveal the direction and behaviour of late-Foxe ice flow through the fiords. The presence of undisturbed elongated landforms within the fiords suggests that ice streams have probably been active until the late stage of deglaciation. Landforms transverse to ice-flow direction include grounding-zone wedges, frontal moraines, grounding-line fans, recessional moraines and De Geer moraines. These landforms are interpreted as the result of former standstills of the ice margin during deglaciation. The occurrence of grounding zones in deep (>800 m) part of the fiords contrasts with studies suggesting instability and rapid retreat of outlet glaciers over deep fiord basins. Sediment-filled basins, often characterised by the presence of turbidity channels, gullies and mass movement scars occur in-between the moraines. Sediment-filled basins with a ponded architecture between sills illustrate that most of the sediment accumulation was ice-proximal during deglaciation and characterised by gravity-driven flows. The proposed landform-assemblage model for northeastern Baffin fiords includes landforms typical of different fiord landsystems.

© 2019 Elsevier B.V. All rights reserved.

1. Introduction

The Greenland Ice Sheet (GrIS) and other glaciers located around the Arctic Circle have been increasingly losing mass during the last decade, thereby contributing to global sea-level rise (Gardner et al., 2011, 2012, 2013; Rignot et al., 2011). The link between the interior of these continental ice masses and the ocean generally takes the form of marine-terminating outlet glaciers. The GrIS loses up to 50% of its ice mass through calving of its outlet glaciers (van den Broeke et al., 2009; Rignot et al., 2011; Shepherd et al., 2012). Hence, tidewater glaciers play an important role in the stability of ice masses (Joughin et al., 2012). Marine-terminating outlet glaciers generally flow through fiords, which are glacially overdeepened estuaries (Syvitski et al., 1987; Syvitski and Shaw, 1995). A recent study using radar-derived ice thickness measurements and bathymetry under the GrIS highlighted the influence of fiord bathymetry on ice flow, grounding line migration, calving dynamics, and subglacial drainage (Morlighem et al., 2017);

fiord sills act as 'protectors' for the incursion of warm waters under outlet glaciers, while landward retrograde beds and overdeepened basins make a greater part of glaciers vulnerable to ocean forcing. Indeed, studies suggest that glaciers resting on reverse-bed slopes may potentially be unstable (Mercer, 1978; Schoof, 2007; Joughin and Alley, 2011; Morlighem et al., 2017) and retreat over deep fiord bathymetry may trigger catastrophic retreat (Briner et al., 2009a). However, recent modelling studies reveal that grounding of glaciers can be achieved on reverse-bed slopes (Nick et al., 2010; Gudmundsson et al., 2012). Other studies also suggest that it is the width variations of a fiord or a trough that play a key role in the stability or instability of the ice margins in the marine environment (Jamieson et al., 2012; Carr et al., 2013a). These divergent findings demonstrate that knowledge of long-term glacial retreat dynamics in fiords and troughs remains limited. Considering that the ice mass of the GrIS could account for >7 m of global sea-level (Morlighem et al., 2017), there is a need to better understand the dynamics of retreat of outlet glaciers in fiord settings in order to provide accurate predictions of the long-term evolution of ice sheets and of glacio-eustatically driven sea-level rise.

While recent satellite data bring insights on ice-sheet dynamics on a decadal scale, they do not provide a long-term overview of their

* Corresponding author.

E-mail addresses: etienne.brouard.1@ulaval.ca, [\(E. Brouard\).](mailto:brouard.etienne@courrier.uqam.ca)

evolution. One way to provide data on centennial to millennial evolution of outlet glaciers in fiord systems is to investigate formerly glaciated systems. The study of inherited glacial geomorphology in fiords is, therefore, critical to our understanding of ice sheets and the behaviour of their outlet glaciers. The geomorphology of fiords has consequently been the object of numerous studies, which uncovered a number of landforms and processes linked to glacial and postglacial environments (e.g., Syvitski et al., 1987; Syvitski and Shaw, 1995; Howe et al., 2010; Dowdeswell et al., 2016). The seabed geomorphology of fiords has also been documented using high-resolution bathymetric imagery (e.g., Ottesen and Dowdeswell, 2009; Dowdeswell and Vásquez, 2013; Hjelstuen et al., 2013; Dowdeswell et al., 2014; Hodgson et al., 2014; Flink et al., 2015; Batchelor et al., 2017). From these studies, different glacial landsystems, in the form of schematic models, have been proposed to identify processes and conditions that prevailed in fiords (Powell, 2003; Dowdeswell and Vásquez, 2013; Dowdeswell et al., 2016; Batchelor et al., 2017). In a similar way to those systems, the Canadian Arctic was almost entirely covered by glacial ice during the Last Glacial Maximum, with continental margins comprising numerous fiords (Syvitski et al., 1987; Dyke, 2004). In the eastern Canadian Arctic, Eastern Baffin Island represents a valuable target for the study of fiords glacial geomorphology as it is characterised by fiords that were occupied by outlet glaciers of the Laurentide Ice Sheet (LIS) during deglaciation (Andrews and Ives, 1978; Miller et al., 2002; Dyke, 2004; Briner et al., 2009a). Northeastern Baffin Island fiords are also carved in a coastal mountain range, which is similar to the location of modern GrIS ice margins. Understanding the retreat dynamics of the LIS through northeastern Baffin Island fiords can therefore provide a relevant paleoglaciological analogue for predicting future GrIS dynamics related to climate change.

In this paper, we document and interpret the seabed glacial to post-glacial geomorphology of three major fiord systems of northeastern Baffin Island based on newly acquired high-resolution swath bathymetry imagery. We propose a conceptual landsystem model for the landform assemblages of these fiords, which has implications for: 1) ice streaming in fiord systems; 2) the factors contributing to the stability of the ice margin; and 3) the controls on sedimentation.

2. Regional setting

2.1. Geology and physiography of the fiords

The studied fiords along the northeastern Baffin Island Coast are grouped into three larger fiord systems that are connected to a cross-shelf trough on the continental shelf (Fig. 1): Clark, Gibbs and Sam Ford fiords are connected to Scott Trough (grouped here as Scott fiords; Brouard and Lajeunesse, 2017); Cambridge, Quernbitder and Dexterity fiords are connected to Buchan Trough (Buchan fiords); and Erik Harbour, Milne Inlet, Oliver Sound and Eclipse Sound are connected to Pond Trough (Pond fiords). Scott and Buchan fiords were glacially excavated into Archean crystalline rocks of the Rae Craton (2.2–1.8 Ga; Jackson and Berman, 2000). The resulting physiography of Scott and Buchan sectors is an alternating pattern of high peaks (1000–1900 m) and incised glacial valleys that form the fiords. In the Scott fiords system, Clark Fiord is ~90 km long and up to 720 m deep, while its width varies from 2 to 10 km. Clark Fiord is connected south to Gibbs Fiord between Sillem and Scott islands and by a 100–200 m-deep arm between Baffin and Sillem islands (Fig. 1). Gibbs Fiord is ~92 km long and ~705 m deep. Its width varies between 1.5 km at its head and 8.5 km at its mouth. South of Gibbs Fiord, Sam Ford Fiord is ~110 km long and >900 m deep. Its width varies from 3 km at its head to 10 km at its mouth. To the west of Sam Ford Fiord, Walker Arm is connected perpendicularly to the main trunk of Sam Ford Fiord. Walker Arm shows a 90° bend after ~15 km of the junction to Sam Ford Fiord and extends for 40 km in parallel to Sam Ford Fiord (Fig. 1).

The physiography of the Buchan fiord system is similar to Scott fiords: Cambridge, Quernbiter, Dexterity and Tromso fiords are incised in the middle of a plateau of high peaks (1000–1250 m) covered by icefields (Fig. 1). The major difference between the two sectors is the presence of a gulf (Buchan Gulf) and inlets (Patterson Inlet) between the mouth of the fiords and the continental shelf. Buchan Gulf is a 36 km long and 14 km wide sound with depths >800 m. To the southwest of Buchan Gulf, Cambridge Fiord is 64 km long and between 2 and 4.5 km wide. Cambridge Fiord is characterised by 5 basins that reach 750 m in depths separated from each other by bedrock and morainic sills (Stravers and Syvitski, 1991). To the west of Buchan Gulf, Quernbiter Fiord is 35 km long, with a width varying from 1.6 to 5.5 km and a depth of 750 m. Southeast of Buchan Gulf is the complex fiord system in which Paterson Inlet and Dexterity Fiord interconnect. Dexterity Fiord is relatively narrow (0.5–5 km) but extends over 97 km.

To the north, the fiords of the Pond system were excavated in a more complex geological setting (Fig. 1). The area is divided into three distinct geological formations: the eastern part of the system, Eclipse Sound and Pond Inlet, crosses Archean metamorphic rocks of the Dexterity Belt (Jackson and Berman, 2000) and Cretaceous sedimentary rocks (Eclipse Trough; Faber et al., 1989); and the western part of the Pond system is included in Mesoproterozoic sedimentary rocks of the Borden Basin (1.27–1.19 Ga; Jackson and Berman, 2000; Fig. 1). Located south of the convergence between Navy Board Inlet and Eclipse Sound, Milne Inlet extends in a N-S orientation over 80 km and has a width reaching ~20 km. Formed by the convergence of several smaller inlets and bays, Milne Inlet is >840 m deep. It is also characterised by the presence of several islands and is divided into two fiord arms in the south. In the east, the fiords of Oliver Sound and Erik Harbour are located in the orogeny of Committee (2.9–2.7 Ga; Jackson and Berman, 2000). Oliver Sound forms a 73 km long fiord which width varies from 1 to 7.3 km. Oliver Sound reaches >400 m in depths and has three fiord arms to the south. Milne Inlet and Oliver Sound meet in Eclipse Sound. Eclipse Sound separates Baffin Island from Bylot Island on a distance that varies between 13 and 35 km. Eclipse Sound is >1000 m deep and is bounded to the northeast by Navy Board Inlet and to the east by the Pond Inlet (Pond Trough). Finally, Erik Harbour is a 12 km long N-S-oriented fiord; it is 2 to 5 km wide and ~300 m deep.

2.2. Foxe Glaciation and deglaciation

During the Last glacial episode (29–16 cal ka BP), the three fiord systems of northeastern Baffin Island were inundated by the LIS that extended to reach the shelf break at the mouth of the troughs (Brouard and Lajeunesse, 2017). Deglaciation of the continental shelf was completed by ~15–12 cal ka BP as coastal forelands emerged from ice (Briner et al., 2005, 2006) and LIS outlets retreated to the fiord mouths. Postglacial sedimentation has been prevailing in the troughs from at least ~12 cal ka BP and probably up to 15 cal ka BP, which marks a minimum age for presence of outlets at the fiord mouths (Osterman and Nelson, 1989; Praeg et al., 2007). Outlet glaciers of the LIS occupied the entire fiords until ~11.4 cal ka BP (Dyke, 2004) before rapidly retreating inland towards the fiord heads (Briner et al., 2009a). Cosmogenic and radiocarbon ages in Sam Ford Fiord indicate that the fiord was mostly deglaciated by 9.3–9.1 cal ka BP, but only completely deglaciated by ~7 cal ka BP (Briner et al., 2009a). This rapid deglaciation roughly corresponds to the early Holocene (10–8.5 cal ka BP) peak in temperature (linked to summer insolation) recorded in nearby lakes (Miller et al., 2005; Briner et al., 2006) and across Baffin Bay (Briner et al., 2016). The outlet glaciers retreat was halted during the 9.5–8 cal ka BP interval which led to the construction of the extensive (>1000 km long) Cockburn moraine complex, which is apparent across most of Baffin Island (Andrews and Ives, 1978). Following the Cockburn Substage (9.5–8 cal ka BP), retreat of the LIS outlets from the fiords was completed by 7 cal ka BP (Dyke and Hooper, 2001; Dyke, 2004;

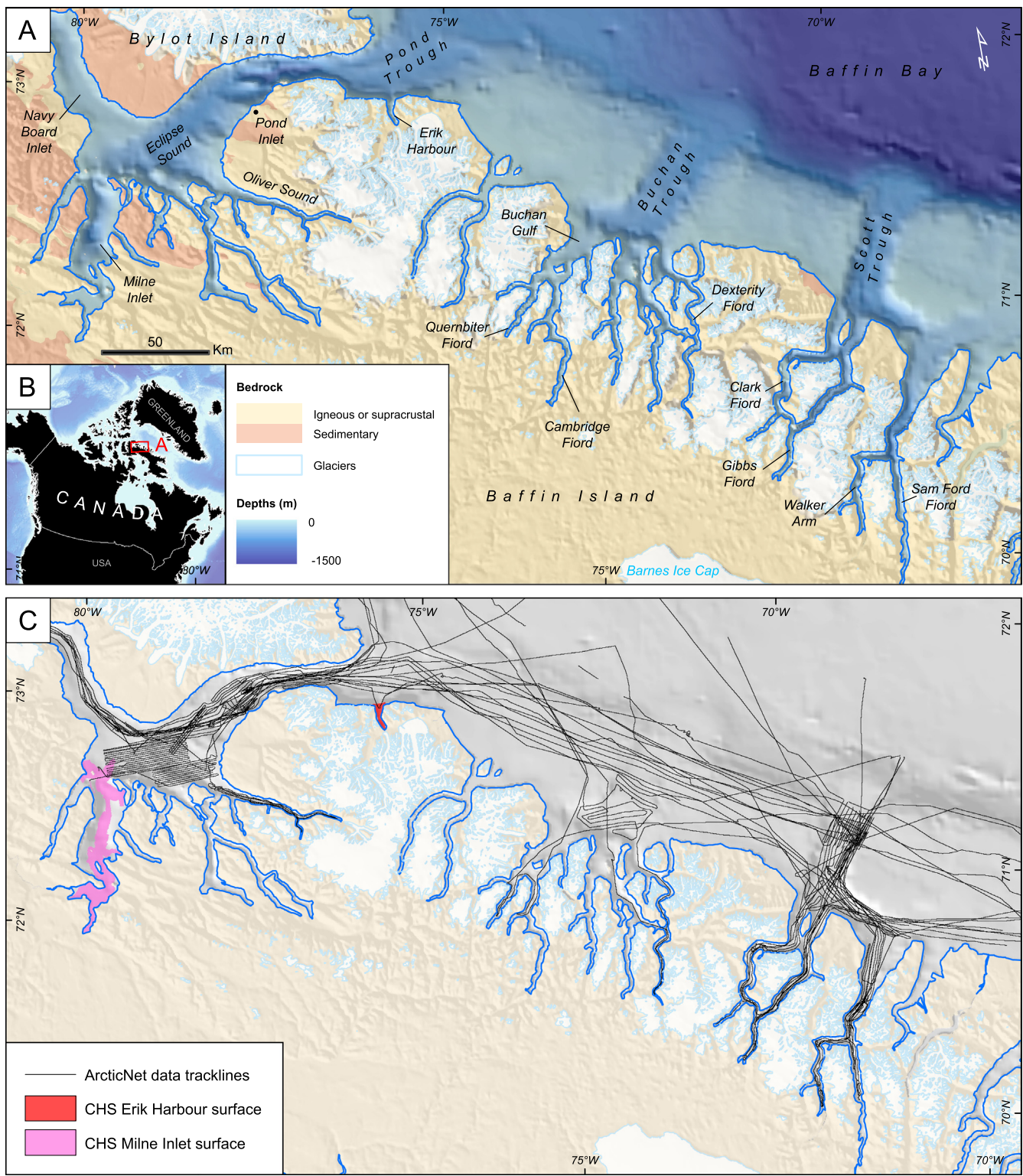


Fig. 1. A. Physiography and bathymetry of the northeastern Baffin Island fiords. B. Location of the study area. C. Ship tracks of the ArcticNet expeditions and areas of surfaces provided by the Canadian Hydrographic Service.

Briner et al., 2009a). All fiords described here, except for Milne Inlet, are today under the influence of small glaciers from local ice caps present on the high summits (Fig. 1). A recent study in Ayr Lake Valley, just south of Sam Ford Fiord, indicates that glaciers that drained local ice caps were more extensive during the Cockburn Substage than during the Younger Dryas. These glaciers did not readvance further than their position reached during the 8.2 ka cold event (Young et al., 2012) but

readvanced during the Little Ice Age and then retreated slowly to their present-day position (Briner et al., 2009b).

3. Materials and methods

The analysed multibeam bathymetry database is a compilation of the ArcticNet and the Canadian Hydrographic Service (CHS) bathymetry

databases (Fig. 1). For the ArcticNet database, multibeam bathymetric data were collected using Kongsberg EM-300 and EM-302 (30 kHz) echosounders onboard the CCGS Amundsen by the Ocean Mapping Group (2003–2013, University of New Brunswick) and the Laboratoire de Géosciences Marines (2014–2016, Université Laval). The specifics of acquisition for each expedition can be obtained from Géoindex+ (www.geoindex-plus.bibl.ulaval.ca) and from Ocean Mapping Group websites (www.omg.unb.ca/Projects/Arctic/ArcticMetadata.html). The multibeam bathymetry data were processed using Caris Hips & Sips and MB-System softwares. ArcticNet data were gridded at a 10 m-grid resolution for interpretation and analyses. The CHS swath bathymetry data comprise surfaces for Milne Inlet and Erik Harbour at 5 m-grid resolution. The specifics of acquisition can be obtained via a CHS Info request (CHSInfo@dfo-mpo.gc.ca). Data visualisation and mapping were realised using ESRI ArcGIS 10.2 software. ArcticNet seismic reflection data were acquired using Knudsen K320R and 3260 3.5 kHz Chirp systems and were interpreted using the NRCan SegyJP2Viewer software (Courtney, 2013). National Resources Canada (NRCan) seismic reflection data was acquired through the NRCan Marine Data Holdings public database and were visualised and analysed using the LizardTech GeoViewer software. Maps and seismic reflection data were transferred to the Adobe Photoshop CS5 software for figure production and editing. Seismic reflection data were enhanced using the Brightness/Contrast tool in Adobe Photoshop CS5 for a clearer visualisation. The International Bathymetric Chart of the Arctic Ocean data (IBCAO; Jakobsson et al., 2012) at a 500 m-grid resolution was used for large-scale overview of the continental shelf and for map production.

4. Results

4.1. Subglacial landforms

Fiords are glacially eroded landscapes that commonly bear traces of palaeo-ice-flow activity on their floor and walls (Holtdahl, 1967). Numerous elongated landforms oriented along the fiords axis occur in the northeastern Baffin fiords and reflect variations in ice-flow direction and velocity. Subglacial landforms include mega-scale glacial lineations (MSGL), drumlins, crag-and-tails, grooves and meltwater channels.

4.1.1. Mega-scale glacial lineations (MSGL)

Clusters of elongated, linear to curvilinear landforms are documented in Clark and Gibbs fiords, as well as in Eclipse Sound and Milne Inlet (Fig. 2). In each cluster, these ridges have a parallel or convergent orientation. Individual ridges occur in most of the other fiords and in association with drumlins, grooves and crag-and-tails. Up to 7.1 km long and up to ~390 m wide, these ridges have apparent elongation ratios of >10:1. The vast majority of these landforms have a smooth and mostly regular texture, which probably reflects their sedimentary character (Fig. 2E). In some cases, ridges have a rougher texture that probably reflects bedrock character and a very thin sediment cover (Fig. 2E). These ridges are interpreted as MSGLs formed subglacially under an ice stream (Clark, 1993; Stokes and Clark, 2002). MSGLs have been documented in other marine and terrestrial settings (e.g., Livingstone et al., 2012; Margold et al., 2015a) and are interpreted as indicators of fast ice flow and palaeo-ice stream activity (e.g., Clark, 1993; Stokes and Clark, 2002). In the Canadian Arctic, submarine MSGLs have mostly been identified on the floor of glacial troughs, but also in fiords and sounds (e.g., Bennett et al., 2015; MacLean et al., 2016a, 2016b, 2017; Brouard and Lajeunesse, 2017). The occurrence of MSGLs has also been inferred under the convergent ice-stream flow in a fiord below the present-day GrIS (Jezek et al., 2011).

4.1.2. Drumlins

Oval-shaped landforms are often present in association with MSGLs (Fig. 2). These landforms have distinct stoss and lee sides and are found in clusters. These landforms have lengths of <1.9 km, widths of <600 m,

and apparent elongation ratios of <1:10. They mostly occur on fiord mouth sills or on bathymetric highs (Fig. 2). They have geometries and morphologies similar to drumlinoid landforms described extensively in formerly glaciated areas; they are generally interpreted to be formed subglacially (e.g., Clark et al., 2009; Jakobsson et al., 2016). Accordingly, these landforms are interpreted as drumlins. While the processes behind the formation of drumlins remain open to debate (e.g., Menzies, 1979; Stokes et al., 2011; Eyles et al., 2016), they are interpreted to record former direction of ice flow (King et al., 2007; Clark et al., 2009). Drumlins preserved on the seafloor of the fiords of northeastern Baffin Island have orientations consistent with assumed ice flow, i.e., along and parallel to the general orientation of each fiord. Some drumlins are characterised by the presence of an overdeepened curvilinear depression in front of their stoss side (Fig. 3A–B), which are similar to ‘crescentic scours’ observed on palaeo-ice stream beds in Antarctica and Greenland (Graham et al., 2009; Graham and Hogan, 2016; Fig. 3B). Although the origin of these crescentic scours has still not been defined, the most plausible hypothesis is that these channel-like landforms were produced by meltwater-induced erosion.

4.1.3. Grooves

Linear to curvilinear negative landforms occur in sediments or in bedrock in Clark Fiord, Eclipse Sound, Milne Inlet and Oliver Sound (Fig. 2). These landforms are oriented in the fiord axis (flow-oriented) direction and have lengths of <5.4 km with widths of <170 m. Similar landforms have been described in ice-stream tracks in palaeo-settings (Bradwell et al., 2008; Graham et al., 2009; Bradwell, 2013; Krabbendam et al., 2016) and under modern ice streams (King et al., 2007, 2009; Jezek et al., 2011). These landforms usually occur beside MSGLs and/or drumlins (Fig. 2) and are interpreted as grooves produced by keels beneath glacial ice eroding the underlying substrate.

4.1.4. Crag-and-tails

Flow-oriented landforms with identifiable bedrock ‘crag’ at the head and a drift tail, forming typical crag-and-tails (Evans and Hansom, 1996) were previously described in the study area (Bennett et al., 2015). The crag-and-tails on Eclipse Sound seabed form along concentric arcs of bedrock ridges suggesting convergent ice flow under an ice stream flowing east towards Pond Trough (Bennett et al., 2015; Dowdeswell et al., 2016a; Fig. 2B–F). In addition to Eclipse Sound crag-and-tails, series of elongated sediment tails extending from bedrock ridges are present in most of the fiords of northeastern Baffin Island. Most are positioned on or seaward of the sill at fiord mouths (Fig. 2) or occur downslope of bedrock outcrops. They have lengths <3.8 km and widths <570 m, and are generally present beside MSGLs, drumlins and grooves. Sediment tails are interpreted to result from groove-ploughing under glacial ice on the lee side of a bedrock outcrop alike typical crag-and-tails (Clark et al., 2003). As with drumlins, overdeepened curvilinear depressions are present upstream of some crag-and-tails (Fig. 3B).

4.1.5. Meltwater channels

Sets of sinuous longitudinal depressions occur on bathymetric highs at the mouth of Buchan Gulf, Sam Ford Fiord, Gibbs Fiord, Milne Inlet and in Eclipse Sound (Fig. 2). These longitudinal depressions are <4.4 km long, <1.2 km wide and can reach >100 m deep. Some are characterised by a flat bottom reflecting sediment infill (Fig. 3C–D). In the study area, these landforms are highly correlated to bedrock outcrops and are sparse in sediment basins. They form anastomosing networks that are mainly flow-oriented and that often occur in-between ice-flow landforms. The sinuosity of the depressions and the fact that some are not flow-oriented suggest that these depressions were not the product of glacial erosion alone. Similar landforms were described in palaeo-ice stream tracks (e.g., Lowe and Anderson, 2003; Nitsche et al., 2013; Smith et al., 2009) and have been interpreted as the product of subglacial meltwater carrying sediments and eroding in hard bedrock (Krabbendam, 2016).

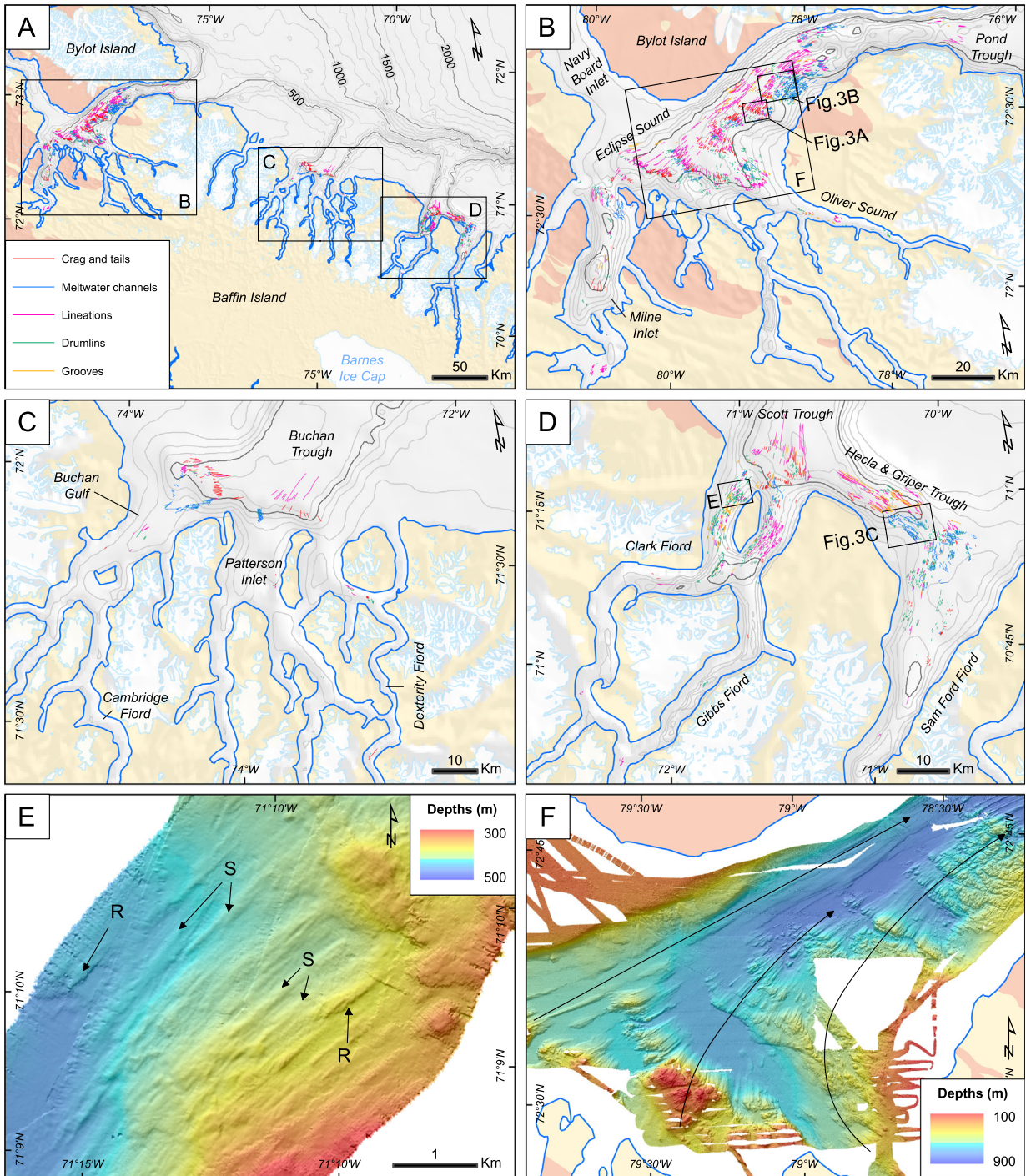


Fig. 2. A. Distribution of ice-flow landforms mapped from swath bathymetry imagery. B. Close-up of distribution of ice-flow landforms in the Pond system. C. Close-up of distribution of ice-flow landforms in the Buchan system. D. Close-up of distribution of ice-flow landforms in the Scott system. E. Examples of mega-scale glacial lineations with rough (R) and smooth (S) character on Clark Fiord sill. F. Overview of bathymetry in Eclipse Sound showing ice-flow oriented landforms converging towards the northeast.

These depressions are accordingly interpreted as meltwater channels formed subglacially under ice-streaming conditions. They reflect abundant meltwater that probably favoured ice-bed decoupling and enable basal sliding and thus ice streaming (Engelhardt et al., 1990; Anandakrishnan and Alley, 1997; Reinardy et al., 2011).

4.2. Ice-marginal landforms

4.2.1. Grounding-zone wedges

Wedges characterised by stoss sides with lower gradients occur in Erik Harbour, Milne Inlet, Eclipse Sound and Sam Ford Fiord

(Figs. 3E and 4). These wedges are perpendicular to the fiord axes and are characterised by numerous iceberg ploughmarks and pits (Fig. 4B–C). Wedges have lengths of 3–13 km with vertical relief reaching up to 150 m. In Sam Ford Fiord, a Chirp subbottom profile over a wedge reveals it is formed of a chaotic, semi-transparent unit. This unit is similar in character to subglacial till forming grounding-zone wedges (GZW) or till sheets (Evans et al., 2005; Ó Cofaigh et al., 2005; Rebisco et al., 2011; Evans and Hogan, 2016) in which MSGs are formed (Heroy and Anderson, 2005; Ó Cofaigh et al., 2005; Evans et al., 2006). These wedge-shaped deposits also have a geometry and a seismic character similar to grounding-zone wedges described in

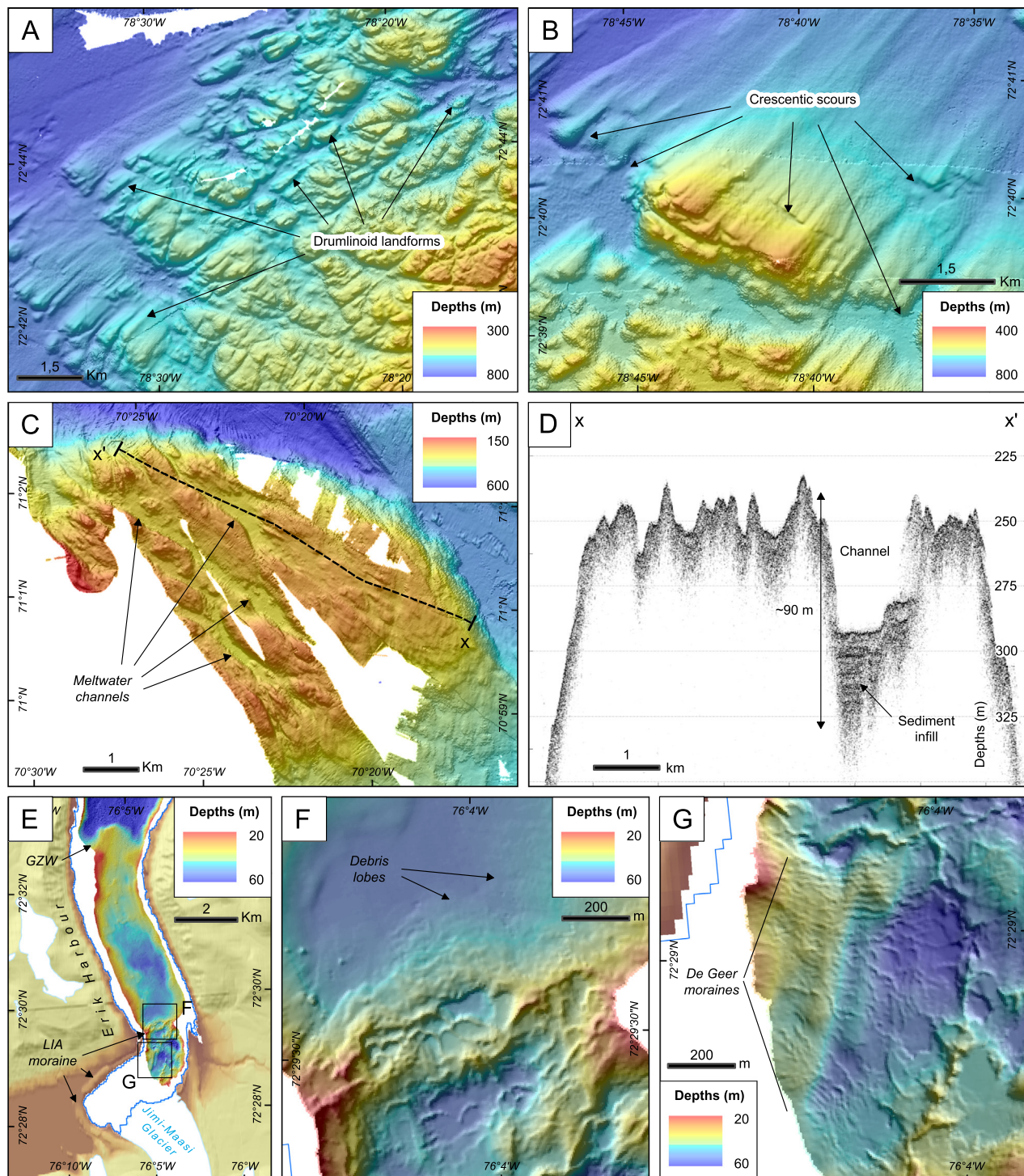


Fig. 3. A. Examples of drumlinoid landforms in Eclipse Sound. B. Examples of crescentic scours around drumlins and crag-and-tails, located in Eclipse Sound. C. Examples of meltwater channels observed on Sam Ford outer bedrock sill. See Fig. 5.2 for legend. D. Chirp profile over a meltwater channel showing a vertical relief to bedrock of at least 90 m and a ~35 m of sediment infill. Profile location is shown on C. E. Swath bathymetry imagery in Erik Harbour. GZW: Grounding-zone wedge. F. Bathymetry of Erik Harbour Head showing LIA moraine and debris flow lobes (DFL). G. Recessional 'De Geer' moraines located iceward of the LIA moraine.

other formerly glaciated systems (e.g., Rebasco et al., 2011; Batchelor and Dowdeswell, 2015; Evans and Hogan, 2016; Lajeunesse, 2016; Batchelor et al., 2017; Lajeunesse et al., 2018) and are thus interpreted as GZWs. Grounding-zone wedges are formed by the accumulation of subglacial sediments at the grounding zone of an ice stream during temporary standstills of an ice margin (Dowdeswell and Fugelli, 2012; Batchelor and Dowdeswell, 2015; Lajeunesse, 2016; Brouard and Lajeunesse, 2017). GZWs have been associated with ice shelves, which

restricts vertical accommodation space for sediments and favour sediment progradation, leading to the formation of low-amplitude and horizontally extensive wedges (Dowdeswell and Fugelli, 2012).

4.2.2. Moraines

In almost all fiords of northeastern Baffin Island, swath bathymetry imagery reveals ridges that are forming elongated, arcuate bathymetric highs oriented transverse to former ice flow (Figs. 4–5). These ridges

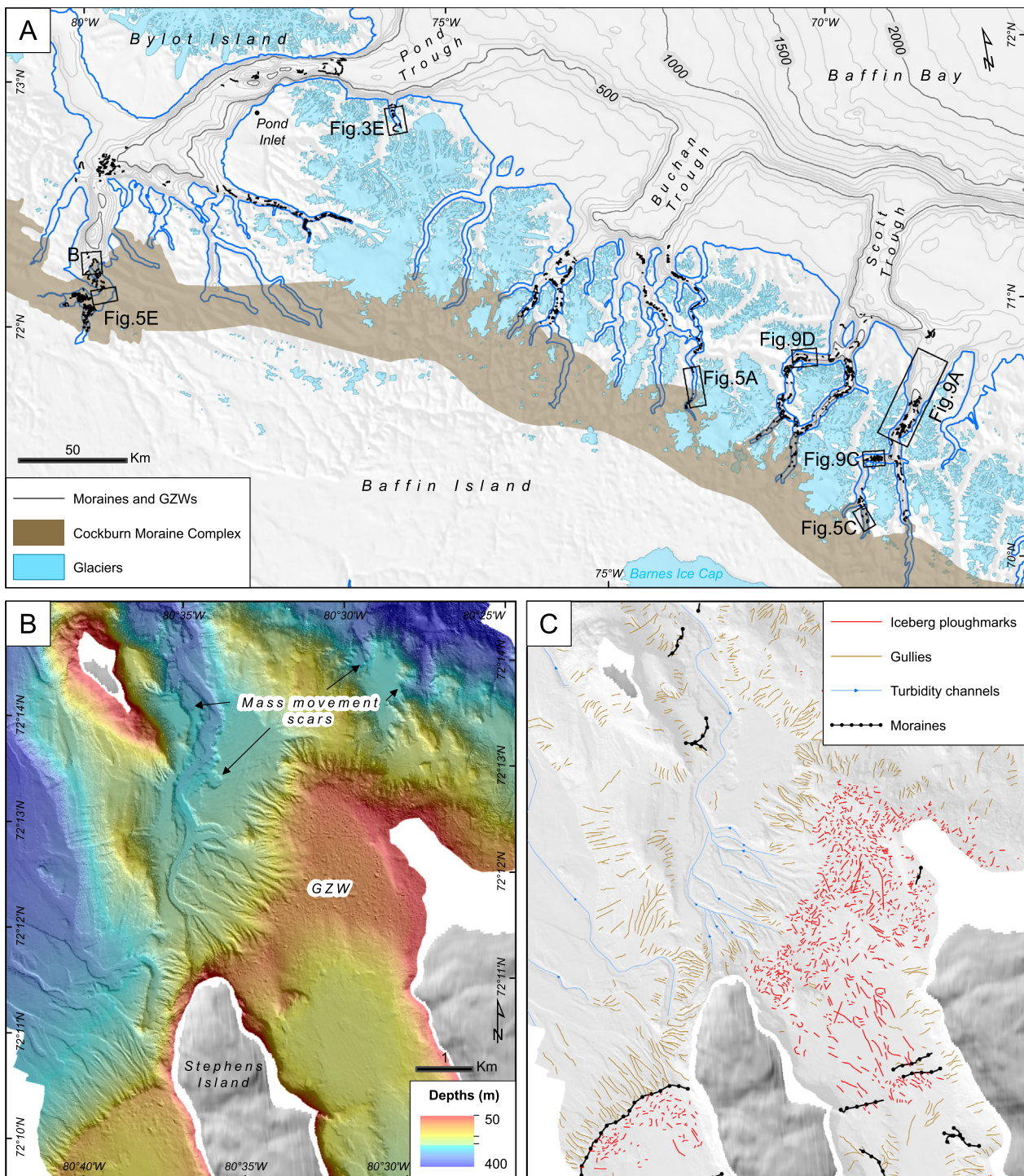


Fig. 4. A. Ice-marginal landforms mapped on bathymetry and the outline of the Cockburn Moraine Complex. B. Swath bathymetry of upper Milne Inlet showing the morphology of the GZW and moraines at the mouth of fiord arms. MMS: Mass movement scar. B. Interpretation of the landforms observed in A.

have lengths reaching <6.2 km and are morphologically steeper up-fjord with more gentle slopes down the fjord (Figs. 3F–4B–5C). Such ridges mostly occur in clusters (Fig. 4A) and at depths <880 m. On Chirp subbottom profiles, these ridges are represented by a strong reflection signal with no penetration, which indicates that they either consists of coarse sediments (>sands), till or bedrock. Ridges are also characterised by iceberg ploughmarks and gullies. The occurrence of ploughmarks and gullies, combined with the near absence of postglacial sediments draping, suggests that these ridges are sediment bodies, most likely representing moraine ridges deposited during standstills

or re-advance of outlet glaciers of the LIS during deglaciation. In Erik Harbour, in front of the present-day Jimi-Maasi glacier, a moraine is observed on land and extends underwater (Fig. 3E). This large moraine ridge is apparent on swath bathymetry imagery together with a set of smaller-scale parallel moraines ice ward. These small moraine ridges are spaced ~25–60 m apart in a regular fashion (Fig. 3G). The parallel and regular spacing character of the small moraines suggest that they are recessional moraines and possibly De Geer moraines. De Geer moraines are usually formed during winter standstills or readvance of the ice margin (Lindén and Möller, 2005; Todd et al., 2007).

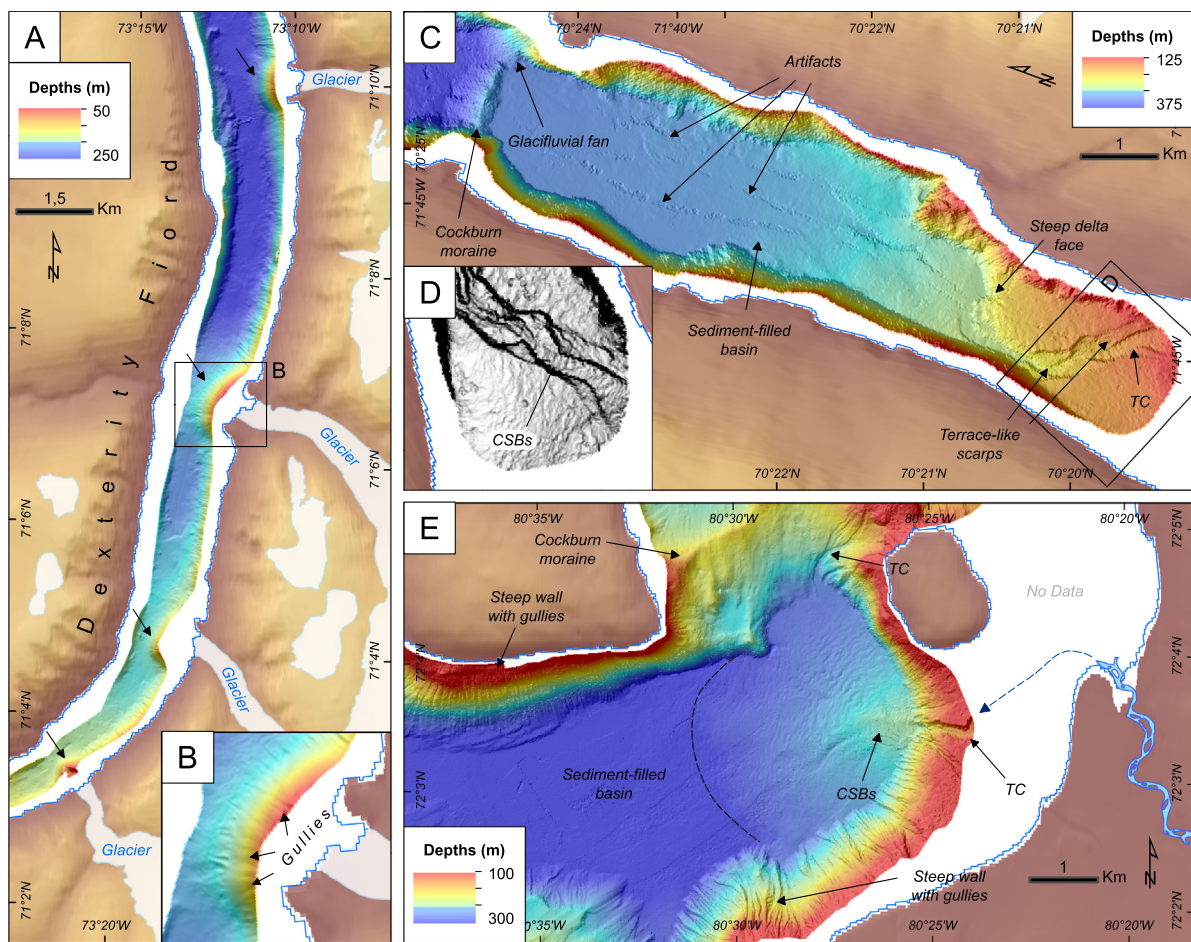


Fig. 5. A. Glaciifluvial fans (GF) in front of ice cap outlet glaciers in Dexterity Fiord. B. Examples of gullies on the steep face of a fan. C. Bathymetry of the head of Walker Arm showing the fiord-head delta characterised by a turbidity-current channel (TC), terraces-like scarps, CSBs and a steep face with mass movement scars. The swath bathymetry also shows a sediment-filled basin ponded between the Cockburn frontal moraine and the fiord-head delta. D. Close-up on the turbidity-current channel and the apparent CSBs. E. Fluvial fan (apparent morphology is highlighted by the dashed line) in Milne Inlet showing CSBs in a turbidity-current channel (TC).

4.2.3. Subaqueous ice-proximal or fluvial fans

Mound-like landforms forming circular bulges have been previously reported from Dexterity Fiord and interpreted as ice-proximal glaciomarine fans (Dowdeswell et al., 2016b; Fig. 5A). Similar bulges occur in nearby Sam Ford, Clark, Gibbs, Quernbiter and Cambridge fiords as well as in Oliver Sound and Milne Inlet. These bulges are generally characterised by gullies forming small channels (Fig. 5B). The bulges are interpreted as subaqueous ice-proximal fans as they are located in front of present-day glaciers and exhibiting a similar geometry to ice-proximal fans in Dexterity Fiord. In Sam Ford Fiord and Oliver Sound, two fans are located directly at the mouth of a marine-terminating glacier and are instead interpreted as ice-contact fans. Fans also occur at the mouth of rivers instead of glaciers. These fans possibly originated as glacially fed fans but are today only fed by river inputs, e.g., in Milne Inlet (Fig. 5E). They are interpreted as composite subaqueous glaciifluvial fans or fluvial fans.

4.3. Other landforms

4.3.1. Fiord-head deltas and sediment-filled basins

Sediment infill characterises most fiord valleys (submarine and subaerial) and is generally linked to fluctuations in relative sea level and sediment inputs (e.g., Corner, 2011; Dowdeswell and Vásquez, 2013; Batchelor et al., 2017). Accordingly, tabular and mostly flat basins filled by sediments are present in all the studied fiord systems and comprise much of the surface area between (morainic and bedrock)

sills (Fig. 5C). Some tabular surfaces are bordered by steep slopes characterised by gullies, turbidity channels and chutes (Fig. 5C-D). These surfaces generally constitute the seaward extent of subaerial delta/sandur plains at the fiords head. The infills are thus interpreted as the result of subaqueous deltaic/fan deposition. The ponded architecture of the sediments interpreted on seismic reflection data reveals similar organisation/architecture of each basin, including the fiord-head basin (Fig. 6). This similarity suggests that every basin has undergone similar sedimentation conditions, i.e., the retreat of the ice margin with a succession of ice-contact, ice-proximal and ice-distal units (Gilbert, 1985).

4.3.2. Turbidity-current channels

Elongated and sinuous depressions occur on fiord-head deltas, on fans, on GZWs and on moraine slopes, and extend downslope in flat, sediment-filled basins (Figs. 4B-C, 5C-D-E). These depressions are <8.1 km long, <420 m wide and <35 m deep. Most of them originate as minor gullies converging to form a collective channel. Some channels bear crescent-shaped bedforms (Fig. 5D-E), which are usually associated with high turbidity gravity-flow events (Paull et al., 2010). The documented channels are similar to other turbidity-current channels such as those described in Monterey Canyon (California; Paull et al., 2011) and in other fiord systems (Syvitski et al., 1987; Syvitski and Shaw, 1995; Dowdeswell and Vásquez, 2013; Batchelor et al., 2017). By their sinuous morphology and their location on slopes, the channels are interpreted as turbidity-current channels formed by underflows or currents transporting sediment downslope. Channels also occur in

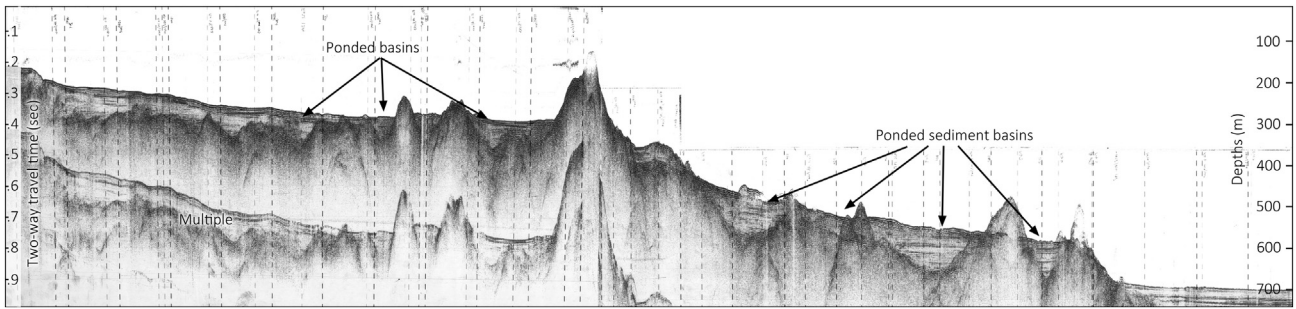


Fig. 6. Airgun seismic reflection profile showing ponded sediments in between morainic and bedrock sills.
Source: Geological Survey of Canada, profile 82031_AG_264_1001.

association with terrace-like landforms (Fig. 4B). These terraces resemble fluvial terraces formed by the erosion and the meandering movement of a river. They are interpreted as the product of erosion caused by a meandering turbidity-current channel.

4.3.3. Mass movement scars

The terrace-like landforms may have been produced by small mass movements triggered by the instability created by the erosion of a meandering turbidity-current channel (Girardclos et al., 2007; Clarke et al., 2014). However, scarps in sediments that are not related to turbidity-current channels also occur in most fiords (Fig. 4B). On the swath bathymetry imagery, they form longitudinal scarps with a lobate character in sediment (Fig. 4B). These scarps are interpreted as mass-movement scars formed by slumps on deltas, fans, GZWs or moraine slopes.

4.3.4. Gullies

While fiord deltas and sediment-filled basins are characterised by scarps in sediment, fiord walls are mostly characterised by small v-shaped linear depressions (Figs. 4B–C, 5B–E) that occur where slope angles are higher than 10°. Generally <50 m large and <10 m deep, these depressions are up to 2.45 km long. Similar landforms are common on high-latitude continental shelves and have also been reported in fiords (e.g., Evans and Dowdeswell, 2016; Batchelor et al., 2017). These landforms are interpreted as submarine gullies formed by sediments eroding the seafloor during their downslope transfer. Since present-day walls are mostly sediment-starved, gullies were probably formed while walls had sediment supply from an ice margin. The sediment accumulations on fiord walls were probably too steep to remain stable under the ice-proximal sedimentation, therefore resulted in small-scale mass movements (Batchelor et al., 2017). The formation of gullies could also be the result of local seismicity, which is fairly active in the Buchan and Scott sectors (Halchuk, 2009; Bennett et al., 2015).

4.3.5. Iceberg ploughmarks

Linear, curvilinear and almost circular depressions with a general random orientation, occur in each fiord. These depressions are up to 2.4 km long, generally <200 m wide (up to ~335 m) and <10 m deep (up to ~15 m; Fig. 7A–B). Similar scours are abundant on high-latitude continental shelves and are interpreted as the product of iceberg keels eroding the seafloor, i.e., iceberg ploughmarks. Here, such scours are present at depths reaching 974 m (Fig. 7B), but the vast majority is located on sills and shallows (Fig. 7A). On sills, the overall orientation of iceberg ploughmarks can be visually inferred and is generally parallel to the ice-flow direction. Modern-day glaciers in the fiords are unlikely to produce icebergs with drafts that will reach >100 m; the thickness of modern glacier tongues is <100 m. Also, modern-day drafts of icebergs flowing through Baffin Bay rarely exceed 300 m (Praeg et al., 2007), indicating that they cannot account for the deep keel scours.

5. Discussion

5.1. Ice-flow patterns

The presence of MSGLs, drumlins, crag-and-tails, and meltwater channels on the seabed indicates that ice streaming has been effective from the early to the late deglaciation stages of the three fiord systems (Fig. 8A). Tributary ice streams of the Scott Ice Stream were interpreted as having been active in outer Sam Ford, Gibbs and Clark fiords (Margold et al., 2015b; Brouard and Lajeunesse, 2017). The presence of ice-flow landforms on the sills indicates that Sam Ford, Gibbs and Clark ice streams remained active when the LIS margin retreated from the continental shelf, most likely as fast-flowing tidewater glaciers. For the Buchan fiords system, the presence of meltwater channels and drumlins on the outer sills suggests that the Buchan fiords were occupied by tributary arms of the Buchan Ice Stream during full glacial conditions and during the deglaciation of the shelf (Brouard and Lajeunesse, 2017). Ice-flow landforms on and landward of the Buchan fiord-mouth sills reflect the presence of fast-flowing tidewater glaciers during the early deglaciation of the fiords. The distribution of ice-flow landforms in Pond fiords shows that ice streaming was effective during the early deglaciation of Pond Inlet, Eclipse Sound, outer Milne Inlet and of Oliver Sound. While ice-flow landforms located in the western part of Eclipse Sound are converging (Bennett et al., 2015; Dowdeswell et al., 2016a), the eastern landforms exhibit diverging orientations around a large bedrock outcrop. Diverging ice-flow landforms suggest that ice was not thick enough to surpass this obstacle, resulting into the division of ice flow into two separate ice-stream arms. The absence of ice-flow landforms on this bedrock high also suggests that ice streaming never occurred over it. Therefore, this bathymetric high may have acted as a sticky spot (Alley, 1993; Stokes et al., 2007) during the entire glaciation cycle. As ice-flow landforms occur on other crystalline bedrock areas in Eclipse Sound, the crystalline character of the bedrock high is unlikely to be the cause for ice-flow divergence. The difference in bathymetry, forming a >500 m 'bump' (or step), is most likely why ice was transported around the high rather than over it. This divergence of ice flow resulted into the formation of an unusual landform which we name a reverse medial moraine (Fig. 8B). Rather than being formed behind an obstacle by converging ice masses, this landform was probably formed by the accumulation of sediments in the void created between diverging ice masses.

As documented in Eclipse Sound, ice streaming occurrence in the three fiord systems does not seem influenced by the nature of the underlying substrate (sediments, sedimentary bedrock or crystalline bedrock). Ice-flow landforms associated with high velocity rates occur over crystalline bedrock and were probably formed by fast ice flow that reached flotation point. The presence of meltwater channels around ice-flow landforms suggests high pressure and volumes of meltwater travelling on bedrock sills under the LIS outlets and fast-flowing outlet glaciers (Krabbendam et al., 2016).

Ice streaming may have been influenced by the geometry of the fiords as it is mostly present in deeper and larger areas

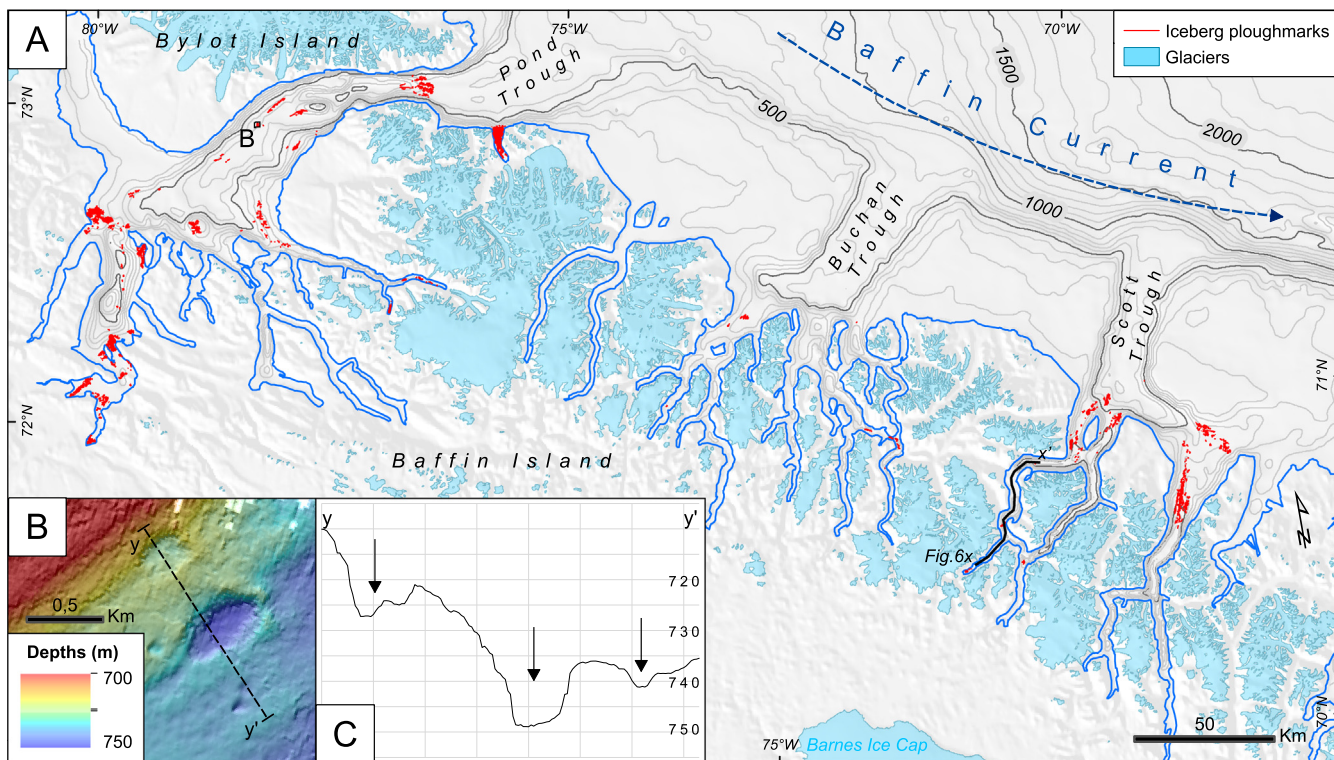


Fig. 7. A. Distribution of iceberg ploughmarks. B. Deep iceberg ploughmarks in Eclipse Sound. C. Bathymetric profile over deep iceberg ploughmarks (arrows shown on B).

(e.g., Eclipse Sound). The relation of ice streaming to fiord basal topography could reflect the glacial-ice volume prone to calving, and reduced lateral-drag-induced buttressing, which together favour rapid retreat and fast ice flow (Schoof, 2007; Jamieson et al., 2012, 2014; Carr et al., 2013b). Conversely, ice-flow landforms are sparse in inner, narrower fiords compared with the outer sills or with Eclipse Sound. Two hypotheses could explain the sparse distribution of ice-flow landforms in inner fiords: i) ice streaming did not occur during the late stage of deglaciation and therefore such landforms were not produced; or ii) ice streaming did occur but the landforms that were produced are buried under the sediment infill in basins and are not visible on swath bathymetry imagery. In the southern part of Milne Inlet, ice streams were probably active during late deglaciation; ice-stream tracks have been identified within the inner fiord (Fig. 2A) and on terrestrial ground just south of both head arms (Milne Ice streams; De Angelis and Kleman, 2007; Margold et al., 2015b; Fig. 8A). Altogether, the continuity in ice-flow landforms in Milne Inlet points out to persistent ice streaming throughout deglaciation. Conversely, no ice stream track has been identified on land, upstream of Scott and Buchan fiords and ice-flow landforms are almost absent in the inner fiords. The absence of ice-flow landforms in Scott and Buchan fiords contrasts with Milne Inlet sector and points towards slow ice velocities during late deglaciation. However, it is surprising that ice streaming did not occur in Scott and Buchan inner fiords, since fiords generally fulfil the two most important criteria for ice streaming, i.e., topography focusing and a calving margin (Winsborrow et al., 2010). Satellite data over Greenland show that present-day velocities are generally high and that ice streaming occurs in fiord settings, even when outlet glaciers are located well inland in the inner part of fiords (Nagler et al., 2015). The occurrence of high velocities in the inner part of present-day fiords suggests that it is possible that ice streaming did occur in inner Scott and Buchan fiords (as in Greenland fiords) but that traces of that activity (ice-flow landforms) were buried under thick sedimentary infill. Therefore, the preservation of these ice-flow landforms on the bathymetry imagery should be dependent of deglacial to postglacial sedimentation. Sedimentation rates are generally higher in ice-proximal settings, thus ice-flow

landforms are most likely to be buried in front of stabilisation landforms such as moraines. On the other hand, a rapid retreat which brings ice-proximal conditions far from the basin should favour a thinner sediment cover and should therefore lead to the preservation of the character of ice-flow landforms on the seafloor. Accommodation space for sediments should influence the burial of the ice-flow landforms in fiord basins. Considering deglaciation with a constant sedimentation rate over two basins of similar depth but different areal extent, the thickness of sediments that can overlay ice-flow landforms will be thinner in the basin with the largest area. Differences in depths are not likely to affect burial because the vertical expression of ice-flow landforms is negligible (few metres) compared to fiord depths (100 s of metres). Burial of ice-flow landforms is then most probable in small surface basins such as fiord-head basins compared to large basins such as Eclipse Sound. Fiord-head basins are today still much influenced by the fluvial sediment input; therefore, the accumulation of sediments in these basins is continuous since deglaciation and favours burial. Finally, mass movement deposits are frequent in fiords and could also lead to the burial of ice-flow landforms. Overall, there are many factors that can lead to the burial of ice-flow landforms in fiords and thus glacial dynamics related to ice flow that occurred during deglaciation may be hard to discern from bathymetric data.

5.2. Stabilizations of the LIS margin and their controls

The occurrence of frontal moraines and GZWs in fiords provides evidence for ice-margin standstills during deglaciation. Ages assessing the onset of deglaciation in fiords remain sparse. For Sam Ford Fiord, it was postulated from cosmogenic and radiocarbon dating that retreat occurred during the 10–9.5 ka BP interval. However, this interval represents a very short time period for the construction of the major moraines seaward of the Cockburn moraine complex. In between the fiords, cosmogenic ages (15–12 ka BP) yield a maximal age for deglaciation of the fiord since coastal forelands are assumed to have deglaciated first. These ages are in accordance with data from Scott Trough which suggest ice-distal sedimentation since at least ~12 ka

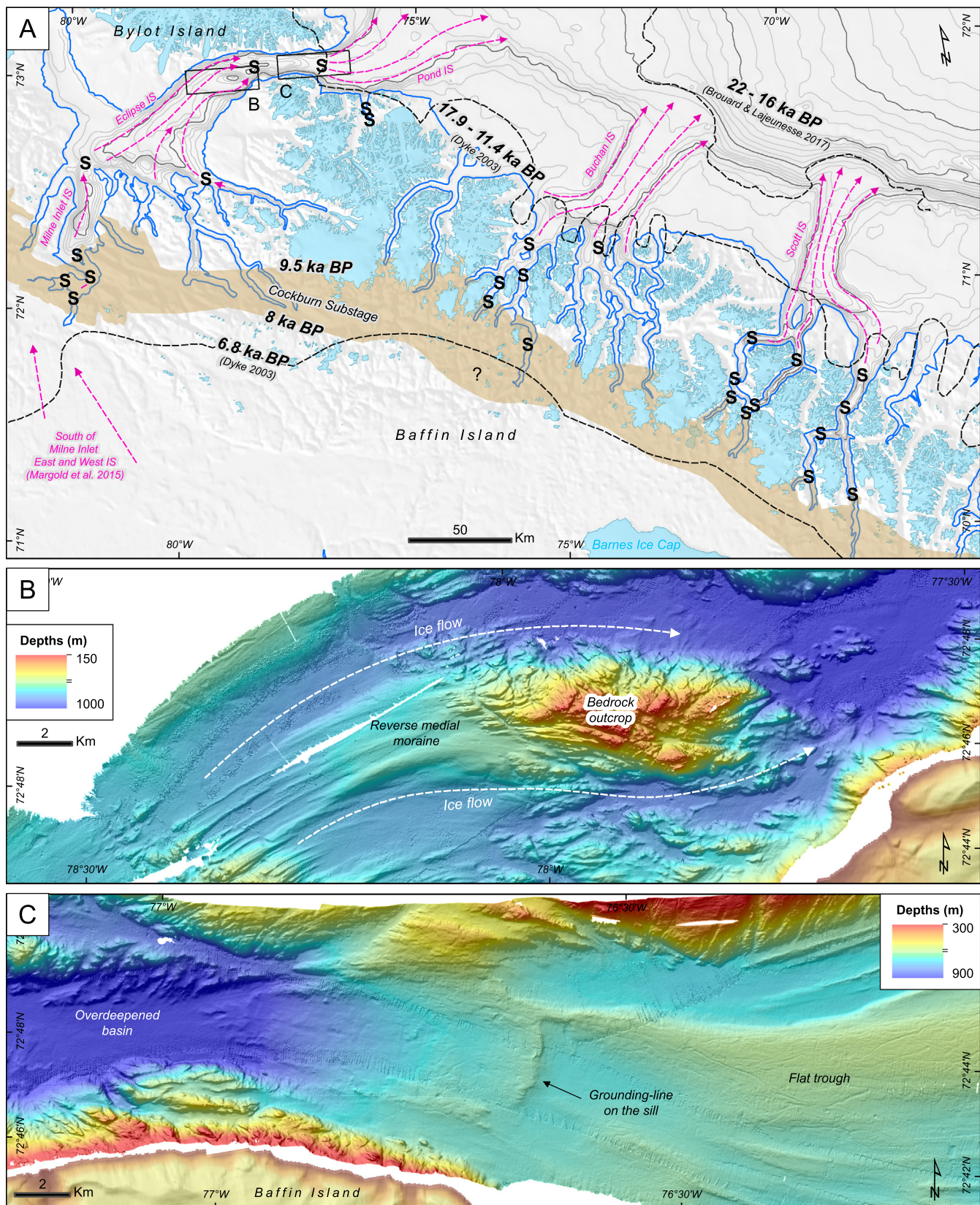


Fig. 8. A. Major ice flows (ice streams; IS), stabilisation (S) and isochrones of deglaciation of northeastern Baffin Island (Dyke, 2004; De Angelis and Kleman, 2007; Brouard and Lajeunesse, 2017). Hatch areas: sedimentary bedrock. B. Reverse medial moraine linked to a bedrock high in Eclipse Sound. C. Grounding-line on Pond Sill showing an overdeepening landward of the sill and a flat cross-shelf trough seaward of the sill.

(Osterman and Nelson, 1989). According to these ages, accumulations of glacial sediments at fiord mouths reflecting the 12–10 ka interval should be observed on the seafloor and most probably on the outer

sills. Except for Pond Inlet (outer Eclipse Sound), the outermost moraines occur far inland (>10 km) of the outer sills. The absence of moraine ridges at the transition between the fiords and the troughs

(except for Pond Inlet) has never been addressed but seems frequent when examining other fiord landsystems; the absence of moraine at the fiord mouth has been reported without further explanations in many landsystems (e.g., Batchelor et al., 2017). Being shallower and restricted in width compared to the troughs, Buchan and Scott fiord-mouth sills represent logical locations for stabilisation, i.e., pinning points. Surprisingly, no traces of stabilisation are observed on these sills. If outlet glaciers stabilised on the fiord-mouth sills of Scott and Buchan fiords, the sediments they carried were probably transferred downslope in the troughs rather than being accumulated on the sills. The outer sill of Pond Inlet contrasts with other outer sills as it is characterised by a moraine ridge rather than a bedrock sill (Fig. 8C). The presence of a moraine ridge on the outer sill of Pond Inlet may be due to the fact that Pond Trough is fairly flat seaward of the moraine. A fairly flat trough implies that the sediments cannot be transported downslope like for Scott and Buchan troughs and, therefore, they accumulate on the sill and form a moraine.

Landward of the outer sills, the first stabilisation is often located where there is a rapid decrease in fiord width. In Sam Ford Fiord, the outermost grounding zone is located on the inner part of the mouth sill, where the fiord is funnel-shaped (Fig. 9A–B). In a similar way, the first moraine in Pond Inlet and the first GZW in Erik Harbour are located where the fiords are funnel-shaped (Fig. 3E). In Clark and Gibbs fiords, the most seaward moraines occur where fiords meet, i.e., between Scott and Sillem islands (Fig. 4A). This transition between a wide fiord to two separate valleys forms a double funnel for ice (Svitski et al., 1987). Other stabilisation deposits also occur at the junction between different fiord arms: e.g., in Milne Inlet, the major GZW associated with the Cockburn moraine complex is located at the transition between a fiord arm and the wider inlet (Fig. 4B). The occurrence of deposits reflecting ice-margin stabilisation in funnel-shape settings suggests a decrease in fiord width that favours ice-margin stabilisation. A similar relation between the stability of the ice margin and the width of the fiord/troughs has also been reported in studies in the Barents/Kara Sea (Carr et al., 2013a) and Antarctica (Jamieson et al., 2012) regions.

In Baffin Island fiords, a decrease in width is, however, not always associated with a stabilisation deposit. The junction between Sam Ford Fiord and Walker Arm is not characterised by a moraine ridge or a GZW. Similarly, the junction of Quernbiter Fiord with Buchan Gulf bears no traces of stabilisation unlike the neighbour Cambridge Fiord (Fig. 4A). The absence of moraines at these junctions, forming funnel-shaped fiords, suggests that a decrease in fiord width alone may not fully account for stabilisation. The examples from Quernbiter and Sam Ford fiords have in common that their junction occurs in the deepest part of the fiord. These overdeepened basins favour rapid retreat as suggested for Sam Ford Fiord (Briner et al., 2009a). Greater depths usually come with greater volume of glacial ice prone to calving (Pelto and Warren, 1991) and in these two cases the volume of glacial ice was probably important enough to overcome lateral support from width decrease. Overall, width and depth represent the vertical area of glacial ice that is marine-terminating and therefore play a role in the overall volume of ice margin prone to calving. The examples from Quernbiter and Sam Ford fiords suggest that ice-margin retreat or stabilisation is more dependent of shifts in the vertical area that is marine-terminating (width * depth) rather than the width variation alone (Meier and Post, 1987).

At depths of >750 m in Sam Ford Fiord, a moraine also occurs where there is no apparent change in depths and widths (Fig. 9A–B). Depths appear to be shallower seaward of the moraine ridge but on Chirp profiles the basin infill appears to be ice-proximal sedimentation (Fig. 9B), suggesting there is no significant variation in depth perceptible. Interestingly, the moraine appears to be attached to the inner corner of the bend in the fiord (Fig. 9A). Moraines extending from the inner corner in bends also occur in Walker Arm and in Clark Fiord; the two occurring in basins >600 m deep (Fig. 9C–D). It is probable that

bends in fiords have the effect of compressing glacier margin and favouring lateral drag, thereby decreasing ice velocities. Since calving rates are coupled to glacier velocities, a bend in a fiord should provide less volume of ice prone to calving. Hence, it could slow retreat and even favour stabilisation.

Alternatively, moraines that have no link with depths, widths or bends could be related to climate (cooling) events. However, it is difficult to assert a climatic origin to moraine ridges without absolute dating. The few ages available for deglaciation indicate that moraines of the Cockburn complex are associated with the 9.5–8 ka BP interval (Andrews and Ives, 1978; Briner et al., 2009a), but the rest of the interval of the deglaciation of the fiords (10–9.5 ka) does not correspond to a cold climate and/or enhanced precipitation. Major moraine ridges located near the fiord head of Clark and Gibbs fiords and in Milne Inlet coincide with the general outline of the Cockburn moraine complex (Fig. 4A); they are therefore interpreted as being constructed during the 9–8.5 ka re-advance of the LIS outlets. Moraines located seaward of Cockburn moraines then probably reflect older standstills during early deglaciation. Considering that glacial ice had left the continental shelf by 15 ka, as suggested by ages on coastal forelands, the extended interval for deglaciation includes the Younger Dryas cold episode. Hence, the outer stabilisation such as those in outer Sam Ford Fiord could have a climatic origin. More ages are, however, needed to assert the timing of the early deglaciation of the fiords.

Finally, more recent moraines deposited by glaciers extending from local ice caps (alpine glaciers) occur in the studied fiords. Alpine glaciers on Baffin Island were more extensive during the Little Ice Age than today and extended near their Cockburn position (Briner et al., 2009b; Young et al., 2012). Judging by their close relation to the present-day position of the glacier, and given the regional glacial history, we infer a Little Ice Age (1375–1820 CE) for the large moraine ridge seaward of the De Geer moraines in Erik Harbour (Fig. 3E). This Little Ice Age moraine could, however, be surimposed on the 8.2 ka moraine and therefore form a composite landform representing both episodes of glacier advance. In any cases, the De Geer moraines represent the slow retreat between the LIA and the present-day position of the Jimi-Maasi glacier.

5.3. Basin fills and sedimentation

The ponded architecture of the sediments in the different basins, as well as the presence of numerous gullies, turbidity-current channels and fans, suggest that sedimentation during deglaciation has been dominated by gravity-driven flows and that suspension plumes and hemipelagic sedimentation were marginal contributors to the total sediment infill volume (Svitski and Shaw, 1995). Ponded sediment fills occur in every fiord and are most obvious where moraine ridges act as barriers to sediment progradation, e.g., in Walker Arm (Fig. 5C). Also, the fact that hemipelagic postglacial sediments do not hide low-amplitude landforms such as iceberg-ploughmarks implies that sedimentation rates by settling plumes were very low after deglaciation (7 ka BP for Sam Ford; 6 ka BP for Milne Inlet; Dyke and Hooper, 2001; Briner et al., 2009a).

The high number of mass-movement scars can also support the hypothesis that much of the sedimentation was not hemipelagic. Three possible triggers can be hypothesised for mass movement in the fiords: i) activity and erosion in turbidity-current channels; ii) a high rate of sedimentation/sediment input on inclined, non-consolidated sediments, or iii) seismicity. Most of the mass-movement scars are located on steep delta, fan or moraine faces where sediment supply in an ice-proximal setting is relatively high. High rates of sedimentation on steep slopes formed in unconsolidated sediments generally result in remobilisation of sediments downslope, a common feature on fans and deltas (Nemec, 2009; Dowdeswell and Vásquez, 2013; Batchelor et al., 2017). In addition, eastern Baffin Island and Baffin Shelf are historically seismically active, with historical events reaching 7.3 in

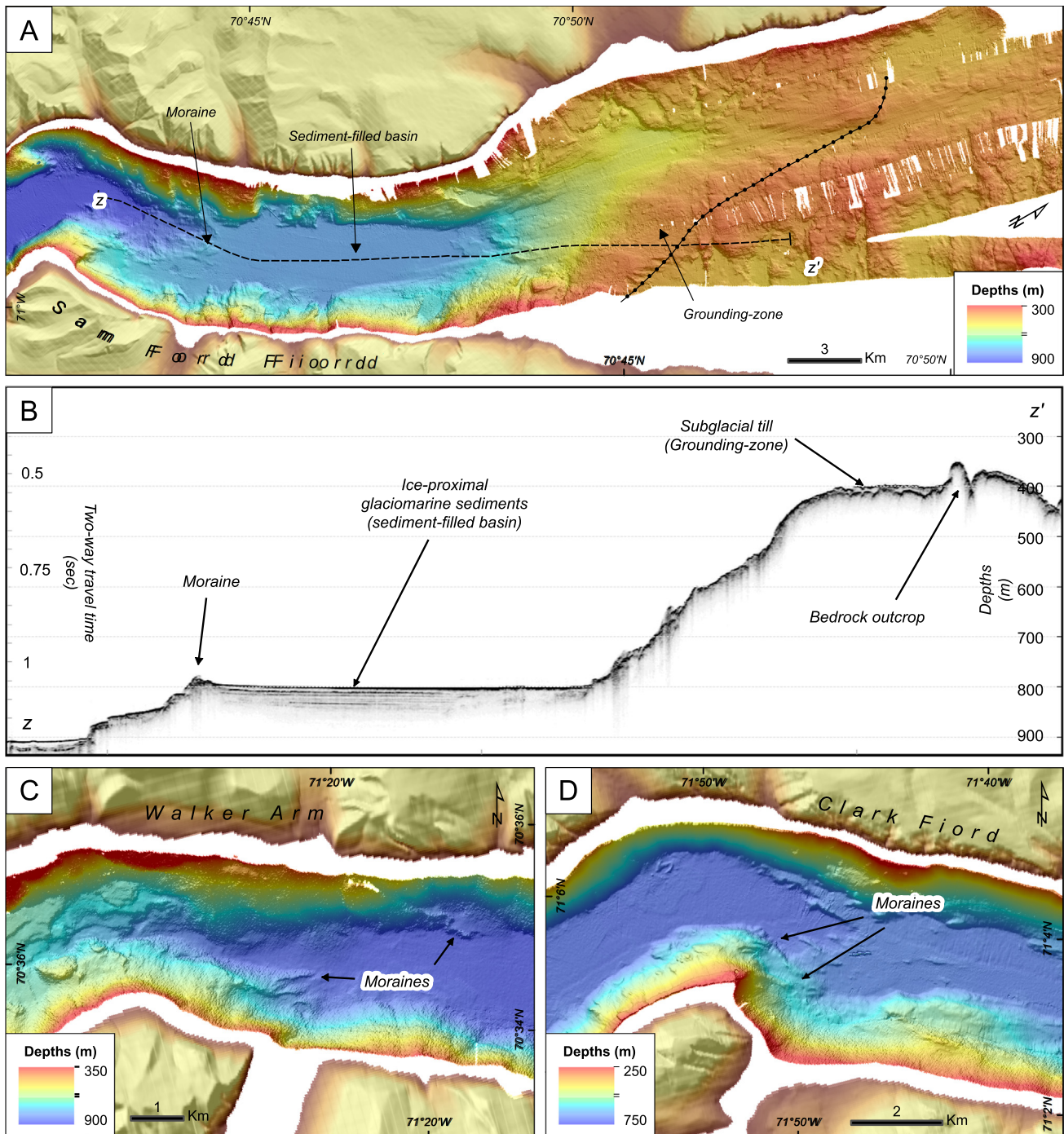


Fig. 9. A. Swath bathymetry of outer Sam Ford Fiord unveiling a grounding zone and a deep moraine/grounding line. B. Chirp profile on outer Sam Ford Sill showing an acoustically transparent unit linked to the grounding zone, a series of high-amplitude reflectors interpreted as ice-proximal glaciomarine sediments, and an impenetrable reflector at the moraine location. The location of the profile is shown on A. C. Moraine ridges linked to a bend in Walker Arm. D. Grounding-zone linked to a bend in Clark Fiord.

magnitude in 1933 (Stein et al., 1979; Hasegawa and Adams, 1990; Bent, 2002), suggesting that mass movement scars observed in the study area could result from seismically-triggered submarine landslides. Recent seismic activity in the northeastern Baffin Island region together with the numerous mass-movement scars and gullies suggest that gravity-driven flows may still contribute to present-day sedimentation.

5.4. Landform assemblage in fiords of northeastern Baffin Island

The study reveals a vast range of depositional and erosional landforms that have a spatial organisation that can be observed in all three fiord

systems of northeastern Baffin Island. Although the fiord systems are separated from each other by hundreds of kilometres, they experienced a similar deglaciation pattern characterised by the inland retreat of the LIS outlet glaciers. This retreat resulted in a landform assemblage that is here simplified into a conceptual model of modern-day seabed expression and geomorphology that can be used in other fiords around the world in order to discern specific retreat dynamics (Fig. 10).

Fiords are generally connected to the troughs on the continental shelf. This transition is generally marked by ice-flow landforms, mainly crag-and-tails, reflecting that fiords acted as tributary ice streams of major collective ice streams that operated in cross-shelf troughs.

Landward of the troughs, the fiord-mouth sills are generally characterised by sedimentary landforms such as MSGLs, or by moraine ridges (e.g., Pond sill moraine). The construction of moraine ridges most likely depends on seaward bathymetry and probably climate forcing, where moraines are most likely constructed landward of a flat (on contrary to overdeepened) trough and during a cold (or precipitation enhanced?) episode.

Landward of fiord-mouth sills, three (3) types of sills can occur: moraines, GZWs or bedrock sills. Major morainic or GZW sills will occur generally in three specific settings: i) where there is a major change in width in the fiord; ii) at the mouth of a fiord arm; or, iii) where there is a bend in the fiord course. The morainic sills or GZWs can also result from climate-related forcing (e.g., Cockburn and LIA moraines) but are generally formed in the three previously detailed settings. In very shallow environments (<60 m), De Geer/recessional moraines can form during winter standstills. The preservation of smaller-scale moraines (such as De Geer or recessional moraines) on the seafloor depends on whether the input (i.e., volume) of sediment in the basin has been high enough since deglaciation to fill the basin and mask their morphology. Unlike moraine ridges that can be constructed in deep (up to 880 m) basins, GZWs mostly form in relatively shallow basins where the development of an ice-shelf together with restricted accommodation space in the basin promote progradation of a sediment wedge. Bedrock sills or outcrops with a similar rough character as fiord-mouth sills can occur in the fiord. The bedrock sills or outcrops are generally overprinted by ice-flow landforms (drumlins, lineations, grooves and meltwater channels) and, less likely, by iceberg ploughmarks. The absence of traces of mass-movement scars or gullies together with a rough texture is generally a good indication of a bedrock sill rather than a morainic sill. Conversely, GZWs and moraines with steep lee slopes generally bear traces of mass movements which take the form of headscarsps, gullies or turbidity-current channels on the upper slope and debris flows at the slope bottom. The occurrence of landforms related to the gravity-driven transport of sediments on moraines and on GZWs is produced by enhanced sedimentation rates, or by (most likely) prolonged sediment influx at one location coherent

with an ice-margin stabilisation. The progradation of these gravity-driven sediment flows is, in most part, stopped when reaching a seaward sill and will settle, filling the basin until the retreat of the ice margin. Therefore, in-between sills, fiord seafloors are characterised by this infill of sediments forming a flat bottom. The formation of flat bottoms in between sills is mostly promoted by ice-proximal sedimentation but postglacial processes such as fluvial sedimentation can contribute to the infill. In fiords no longer occupied by outlet glaciers, the presence of deltaic deposits which form an extension of sandar or fluvial plains reflect the input of postglacial fluvial sedimentation. Fans located in front of glaciers or streams from side valleys can reflect a para/postglacial input of sediments in the basins.

On the sides of sediment-filled basins and of sills, fiord walls are either characterised by fans, by thin sediment cover eroded by small gullies, or by steeply inclined bedrock surfaces. The presence of fans depends on sediment inputs (stream, river or glacier), while the presence of sediments cover on the walls depends on the steepness of the walls, where bedrock walls over 30° slope will prohibit most of sediment accumulation.

Comparing the landform assemblages in fiords of northeastern Baffin Island with other fiord landform-assemblage models, we observe many similarities to fiords of Greenland, Antarctica and Chile. Ice-flow landforms, moraine ridges, GZWs and De Geer moraines are all typical glacially-produced landforms of other fiords landform-assemblage models. The abundance of ice-flow landforms in northeastern Baffin Island fiords is similar to fiords of Greenland or Svalbard (e.g., Batchelor et al., 2017; Forwick et al., 2016) and assemblages in Eclipse Sound are comparable to assemblages in troughs of polar continental shelves (e.g., Graham et al., 2009; Livingstone et al., 2013; Brouard and Lajeunesse, 2017). Ice-proximal or ice-contact fans, fluvial fans and turbidity-current channels are landforms that were also recognized in other fiord landsystems and that are usually associated with high rates of glacial meltwater production (e.g., Dowdeswell and Vásquez, 2013). Finally, the LIA moraine and the De Geer moraines overprinting lineations in Erik Harbour forms a similar assemblage to landforms produced by surge-type glaciers (Ottesen et al., 2008, 2017). Overall, the

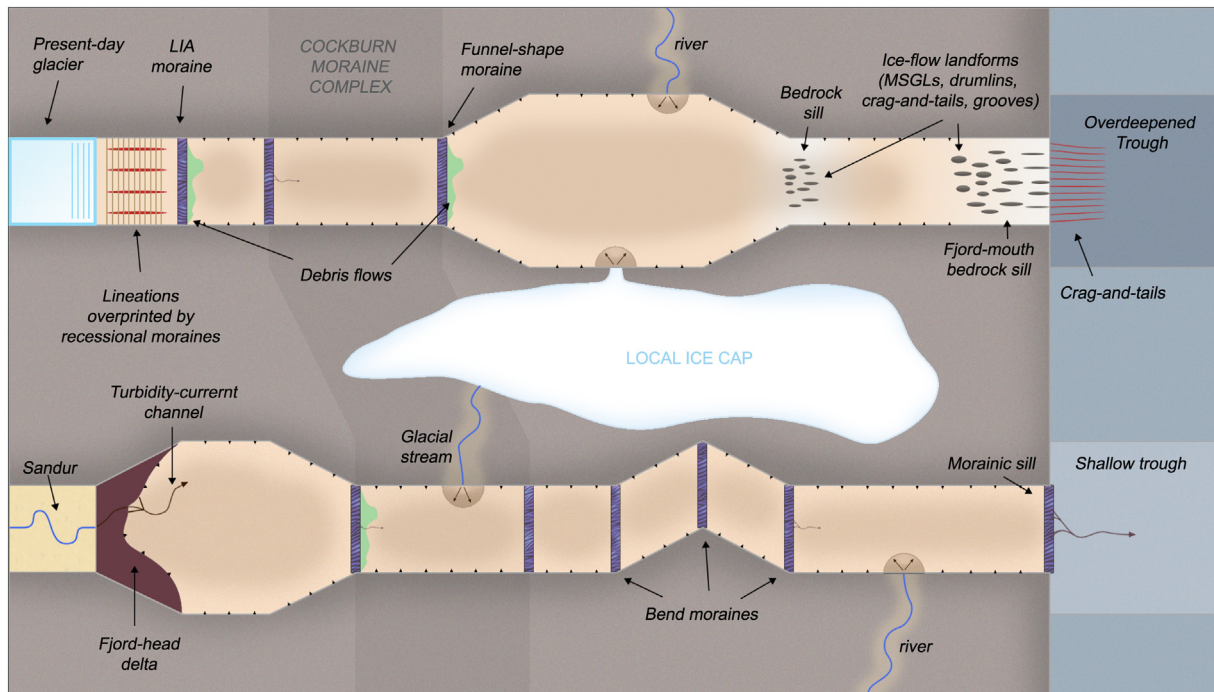


Fig. 10. Conceptual landform-assemblage model for northeastern Baffin Island fiords. The two fiords represent examples of neighbour fiords that have undergone a similar deglaciation but with major differences in seabed geomorphology. These differences are due to various factors such as the depth of the trough, the presence or not of a glacier at the head, the general morphology of the fiords, etc. For detailed description of these factors and context, see Section 5.4. Dark gray rectangles: moraines or GZWs with iceberg ploughmarks. Half circle: fans. Small triangles: gullies.

glacial landsystem in the fiords of northeastern Baffin Island contains landforms characteristic of different landform-assemblage models (glacial landsystems, meltwater-driven and surge-type glaciers). The model presented here thus represents an integrated fiord landsystem model that can apply to discern paleo-ice sheet dynamics of other fiord systems.

The overall landform-assemblage model presented in this study is also a time-transgressive imprint of glacial to postglacial dynamics which reflects a deglaciation of the northeastern Baffin Island that was punctuated by ice-margin standstills, i.e., different stages of landform generation. The first stage is the subglacial generation which includes the ice-flow landforms. The second stage is the ice-marginal generation during which the generation of landforms is mostly dependent of ice-margin movement and therefore dependent of climate forcing and fiord morphology. The third stage is the para/postglacial generation which is dominated by lower sedimentation rates. Every stage of landforms generation also comes with the potential erosion, deformation or burial of landforms produced in previous stages of landform generation which complicates the interpretation of older dynamics from the remaining landforms (i.e., ice streaming in Scott and Buchan fiords). As a result, detailed information on the occupation of ice (subglacial stage) can be difficult to obtain from the analysis of submarine geophysical data.

6. Conclusions

The swath bathymetry imagery and geophysical data collected in three major fiord systems of northeastern Baffin Island reveal in great detail their geomorphology and landform assemblages preserved on the seafloor since deglaciation. The key results of the analysis of these submarine glacial landforms are:

- Landforms observed on the seabed of northeastern Baffin Island outline processes linked to subglacial (glacial lineations, crag-and-tails, drumlins, grooves, meltwater channels), ice-marginal (grounding-zone wedges, moraines, De Geer moraines and fans) or paraglacial (gullies, iceberg ploughmarks, mass movement scars and turbidity-current channels) environments.
- The presence of undisturbed ice-flow landforms within the Milne Inlet suggests that ice streaming was probably active until the late stage of deglaciation. In Buchan and Scott fiords, ice-flow landforms are mostly absent. This absence of ice-flow landforms in the inner part of the fiords is probably due to thick sediment infill which cover most of the fiord basins.
- Divergent ice-flow landforms around bedrock bumps indicate that bathymetric highs acted as sticky spots and therefore as obstacles to fast ice flow.
- The presence of meltwater-channel networks and ice-flow landforms over crystalline bedrock indicates that crystalline bedrock outcrops did not act as sticky spots or obstacles to fast-ice flow, as suggested for other palaeo-ice streams in North America.
- The occurrence of grounding zones of the ice margin in deep (>800 m) part of the fiords contrasts with studies suggesting instability and rapid retreat of outlet glaciers over deep basins. Factors controlling ice-margin stability include funnel-shaped bathymetry, bends and climate.
- Sediment-filled basins generally occur in-between moraines and are often characterised by the presence of turbidity-current channels. These channels indicate that sedimentation in fiords during deglaciation has been dominated by gravity-driven flows.
- Postglacial sedimentation has been dominated by low rates of hemipelagic sedimentation and probably small-scale, seismically-induced gravity-driven flows.

Our landform-assemblage conceptual model proposed for the fiords of northeastern Baffin Island is characterised by different landforms and deposits that form an integrated fiord landsystem that depicts a

complete glacial, paraglacial and postglacial sequence. Documenting this landsystem allows a better understanding of the dynamics of tide-water glaciers in other formerly glaciated fiord systems such as those located elsewhere in the Canadian Arctic Archipelago. Further studies in the northeastern Baffin Fiords should focus on age models to determine ice-retreat rates related to each fiord system.

Data availability

The multibeam bathymetry dataset acquired by ArcticNet can be visualised on the Université Laval Géoindex+ website (<http://geoindex-plus.bibl.ulaval.ca>) and on the Ocean Mapping Group website (<http://www.omg.unb.ca/Projects/Arctic/google/>). The multibeam bathymetry data from the Canadian Hydrographic Survey and the acquisition specifics can be obtained via a CHS Info request (CHSInfo@dfo-mpo.gc.ca). The seismic reflection data along with the acquisition specifics are available on the Geological Survey of Canada website (http://ftp.maps.canada.ca/pub/nrcan_rncan/raster/marine_geoscience/Seismic_Reflection_Scanned/).

Acknowledgements

We sincerely thank the captains, crew and scientific participants (particularly Gabriel Joyal, Annie-Pier Trottier and Pierre-Olivier Couette, Université Laval) of ArcticNet cruises 2014–2016 on board the CCGS Amundsen. We thank John Hughes Clarke and his team at the Ocean Mapping Group (University of New Brunswick) who collected swath bathymetry data in the region between 2003 and 2013. We also thank the Canadian Hydrographic Survey and Glenn Toldi for providing the bathymetric data for the Milne Inlet and Erik Harbour sectors. We thank Martin Roy (UQAM), D. Calvin Campbell (NRCan) and Jean-François Ghienne (CNRS) for providing comments on an earlier version of the paper. This project was funded by ArcticNet Network Centres of Excellence and by an NSERC Discovery grant to P.L.

References

- Alley, R.B., 1993. In search of ice-stream sticky spots. *J. Glaciol.* 39, 447–454.
- Anandakrishnan, S., Alley, R.B., 1997. Stagnation of Ice Stream C, West Antarctica by water piracy. *Geophys. Res. Lett.* 24, 265. <https://doi.org/10.1029/96GL04016>.
- Andrews, J.T., Ives, J.D., 1978. "Cockburn" nomenclature and the Late Quaternary history of the eastern Canadian Arctic. *Arct. Alp. Res.* 10, 617–633.
- Batchelor, C.L., Dowdeswell, J.A., 2015. Ice-sheet grounding-zone wedges (GZWs) on high-latitude continental margins. *Mar. Geol.* <https://doi.org/10.1016/j.margeo.2015.02.001>.
- Batchelor, C.L., Dowdeswell, J.A., Rignot, E., 2017. Submarine landforms reveal varying rates and styles of deglaciation in North-West Greenland fiords. *Mar. Geol.*, 0–1 <https://doi.org/10.1016/j.margeo.2017.08.003>.
- Bennett, R., Campbell, D.C., Furze, M.F.A., Haggart, J.W., 2015. The shallow stratigraphy and geohazards of the Northeast Baffin Shelf and Lancaster Sound. *Bull. Can. Petrol. Geol.* 62, 217–231. <https://doi.org/10.2113/gscpgbull.62.4.217>.
- Bent, A.L., 2002. The 1933 Ms = 7.3 Baffin Bay earthquake: strike-slip faulting along the northeastern Canadian passive margin. *Geophys. J. Int.* 150, 724–736.
- Bradwell, T., 2013. Identifying palaeo-ice-stream tributaries on hard beds: mapping glacial bedforms and erosion zones in NW Scotland. *Geomorphology* 201, 397–414. <https://doi.org/10.1016/j.geomorph.2013.07.014>.
- Bradwell, T., Stoker, M., Krabbendam, M., 2008. Megagrooves and streamlined bedrock in NW Scotland: the role of ice streams in landscape evolution. *Geomorphology* 97, 135–156. <https://doi.org/10.1016/j.geomorph.2007.02.040>.
- Briner, J.P., Miller, G.H., Davis, P.T., Finkel, R.C., 2005. Cosmogenic exposure dating in arctic glacial landscapes: implications for the glacial history of northeastern Baffin Island, Arctic Canada. *Can. J. Earth Sci.* 42, 67–84. <https://doi.org/10.1139/e04-102>.
- Briner, J.P., Miller, G.H., Davis, P.T., Finkel, R.C., 2006. Cosmogenic radionuclides from fiord landscapes support differential erosion by overriding ice sheets. *Bull. Geol. Soc. Am.* 118, 406–420. <https://doi.org/10.1130/B25716.1>.
- Briner, J.P., Binia, A.C., Anderson, R.S., 2009a. Rapid early Holocene retreat of a Laurentide outlet glacier through an Arctic fiord. *Nat. Geosci.* 2, 496–499. <https://doi.org/10.1038/ngeo556>.
- Briner, J.P., Davis, P.T., Miller, G.H., 2009b. Latest Pleistocene and Holocene glaciation of Baffin Island, Arctic Canada: key patterns and chronologies. *Quat. Sci. Rev.* 28, 2075–2087. <https://doi.org/10.1016/j.quascirev.2008.09.017>.
- Briner, J.P., McKay, N.P., Axford, Y., Bennike, O., Bradley, R.S., de Vernal, A., Fisher, D., Francus, P., Fréchette, B., Gajewski, K., Jennings, A., Kaufman, D.S., Miller, G.H., Houston, C., Wagner, B., 2016. Holocene climate change in Arctic Canada and Greenland. *Quat. Sci. Rev.* 147, 340–364. <https://doi.org/10.1016/j.quascirev.2016.02.010>.

- Brouard, E., Lajeunesse, P., 2017. Maximum extent and decay of the Laurentide Ice Sheet in Western Baffin Bay during the Last glacial episode. *Sci. Rep.* 7. <https://doi.org/10.1038/s41598-017-11010-9>.
- Carr, J.R., Stokes, C.R., Vieli, A., 2013a. Recent progress in understanding marine-terminating Arctic outlet glacier response to climatic and oceanic forcing. *Prog. Phys. Geogr.* 37, 436–467. <https://doi.org/10.1177/0309133313483163>.
- Carr, J.R., Vieli, A., Stokes, C., 2013b. Influence of sea ice decline, atmospheric warming, and glacier width on marine-terminating outlet glacier behaviour in northwest Greenland at seasonal to interannual timescales. *J. Geophys. Res. Earth Surf.* 118, 1210–1226. <https://doi.org/10.1002/jgrf.20088>.
- Clark, C.D., 1993. Mega-scale Glacial Lineations and Cross-cutting Ice-flow Landforms. 18 pp. 1–29.
- Clark, C.D., Tulaczyk, S.M., Stokes, C.R., Canals, M., 2003. A groove-ploughing theory for the production of mega-scale glacial lineations, and implications for ice-stream mechanics. *J. Glaciol.* 49, 240–256. <https://doi.org/10.3189/172756503781830719>.
- Clark, C.D., Hughes, A.L.C., Greenwood, S.L., Spagnoli, M., Ng, F.S.L., 2009. Size and shape characteristics of drumlins, derived from a large sample, and associated scaling laws. *Quat. Sci. Rev.* 28, 677–692. <https://doi.org/10.1016/j.quascirev.2008.08.035>.
- Clarke, J.E.H., Marques, C.R.V., Pratomo, D., Vidiera Marques, C.R., Pratomo, D., 2014. Imaging active mass-wasting and sediment flows on a fjord delta, Squamish, British Columbia. *Submarine Mass Movements and Their Consequences*. Springer, pp. 249–260 https://doi.org/10.1007/978-3-319-00972-8_22.
- Corner, G.D., 2011. A Transgressive-regressive Model of Fiord-valley Fill: Stratigraphy, Facies and Depositional Controls. *Incised Val. Time Sp.*, pp. 161–178 <https://doi.org/10.2110/pec.06.85.0161>.
- Courtney, R.C., 2013. Canada GEES 2: visualization of integrated marine geoscience data for Canadian and proximal waters. *Geosci. Can.* 40, 141–148.
- De Angelis, H., Kleman, J., 2007. Palaeo-ice streams in the Foxe/Baffin sector of the Laurentide Ice Sheet. *Quat. Sci. Rev.* 26, 1313–1331. <https://doi.org/10.1016/j.quascirev.2007.02.010>.
- Dowdeswell, J.A., Fugelli, E.M.G., 2012. The seismic architecture and geometry of grounding-zone wedges formed at the marine margins of past ice sheets. *Bull. Geol. Soc. Am.* 124, 1750–1761. <https://doi.org/10.1130/B30628.1>.
- Dowdeswell, J.A., Vásquez, M., 2013. Submarine landforms in the fjords of southern Chile: Implications for glacimarine processes and sedimentation in a mild glacier-influenced environment. *Quat. Sci. Rev.* 64, 1–19. <https://doi.org/10.1016/j.quascirev.2012.12.003>.
- Dowdeswell, J.A., Hogan, K.A., Ó Cofaigh, C., Fugelli, E.M.G., Evans, J., Noormets, R., 2014. Late Quaternary ice flow in a West Greenland fjord and cross-shelf trough system: submarine landforms from Rink Isbrae to Uummannaq shelf and slope. *Quat. Sci. Rev.* 92, 292–309. <https://doi.org/10.1016/j.quascirev.2013.09.007>.
- Dowdeswell, J.A., Canals, M., Jakobsson, M., Todd, B.J., Dowdeswell, E.K., Hogan, K., 2016. *Atlas of Submarine Glacial Landforms: Modern, Quaternary and Ancient*. Geological Society of London.
- Dowdeswell, E.K., Todd, B.J., Dowdeswell, J.A., 2016a. Crag-and-tail features: convergent ice flow through Eclipse Sound, Baffin Island, Arctic Canada. *Geol. Soc. Lond. Mem.* 46, 55–56.
- Dowdeswell, E.K., Todd, B.J., Dowdeswell, J.A., 2016b. Ice-proximal fans in Dexterity Fiord, Buchan Gulf, Baffin Island, Canadian Arctic. *Geol. Soc. Lond. Mem.* 46, 89–90.
- Dyke, A.S., 2004. An outline of North American deglaciation with emphasis on central and northern Canada. *Dev. Quat. Sci.* 2, 373–424. [https://doi.org/10.1016/S1571-0866\(04\)80209-4](https://doi.org/10.1016/S1571-0866(04)80209-4).
- Dyke, A.S., Hooper, J., 2001. Deglaciation of Northwest Baffin Island, Nunavut. Commission géologique du Canada.
- Engelhardt, H., Humphrey, N., Kamb, B., Fahnestock, M., 1990. Physical conditions at the base of a fast moving Antarctic ice stream. *Science* 248, 57–60.
- Evans, J., Dowdeswell, J.A., 2016. Submarine gullies and an axial channel in glacier-influenced Courtauld Fiord, East Greenland. *Geol. Soc. Lond. Mem.* 46, 103–104.
- Evans, D.J.A., Hansom, J.D., 1996. The Edinburgh castle crag-and-tail. *Scott. Geogr. Mag.* 112, 129–131. <https://doi.org/10.1080/14702549608554461>.
- Evans, J., Hogan, K.A., 2016. Grounding-zone wedges on the northern Larsen shelf, Antarctic Peninsula. *Geol. Soc. Lond. Mem.* 46, 237–238.
- Evans, J., Pudsey, C.J., Ó Cofaigh, C., Morris, P., Domack, E., 2005. Late Quaternary glacial history, flow dynamics and sedimentation along the eastern margin of the Antarctic Peninsula Ice Sheet. *Quat. Sci. Rev.* 24, 741–774. <https://doi.org/10.1016/j.quascirev.2004.10.007>.
- Evans, J., Dowdeswell, J.A., Ó Cofaigh, C., Benham, T.J., Anderson, J.B., 2006. Extent and dynamics of the West Antarctic Ice Sheet on the outer continental shelf of Pine Island Bay during the last glaciation. *Mar. Geol.* 230, 53–72. <https://doi.org/10.1016/j.margeo.2006.04.001>.
- Eyles, N., Putkinen, N., Sookhan, S., Arbelaez-Moreno, L., 2016. Erosional origin of drumlins and megaridges. *Sediment. Geol.* 338, 2–23.
- Faber, G.B., MacLean, B., Sonnichsen, G.V., Williams, H., Hoffman, P.F., Okulitch, A.V., Daley, L., 1989. *Geology of the Continental Margin of Eastern Canada*. Geological Survey of Canada.
- Flink, A.E., Noormets, R., Kirchner, N., Benn, D.I., Luckman, A., Lovell, H., 2015. The evolution of a submarine landform record following recent and multiple surges of Tunabreen glacier, Svalbard. *Quat. Sci. Rev.* 108, 37–50. <https://doi.org/10.1016/j.quascirev.2014.11.006>.
- Forwick, M., Dowdeswell, J.A., Laberg, J.S., Ottesen, D., 2016. Glacial landform assemblages in Spitsbergen fjords from the last full-glacial, deglaciation and the late Holocene. *Geol. Soc. Lond. Mem.* 46, 147–150.
- Gardner, A.S., Moholdt, G., Wouters, B., Wolken, G.J., Burgess, D.O., Sharp, M.J., Cogley, J.G., Braun, C., Labine, C., 2011. Sharply increased mass loss from glaciers and ice caps in the Canadian Arctic Archipelago. *Nature* 473, 357–360. <https://doi.org/10.1038/nature10089>.
- Gardner, A., Moholdt, G., Arendt, A., Wouters, B., 2012. Accelerated contributions of Canada's Baffin and Blyot Island glaciers to sea level rise over the past half century. *Cryosphere* 6, 1103–1125. <https://doi.org/10.5194/tc-6-1103-2012>.
- Gardner, A.S., Moholdt, G., Cogley, J.G., Wouters, B., Arendt, A.A., Wahr, J., Berthier, E., Hock, R., Pfeffer, W.T., Kaser, G., Ligtenberg, S.R.M., Bolch, T., Sharp, M.J., Hagen, J.O., van den Broeke, M.R., Paul, F., 2013. A reconciled estimate of glacier contributions to sea level rise: 2003 to 2009. *Science* 340, 852–857. <https://doi.org/10.1126/science.1234532>.
- Gilbert, R., 1985. Quaternary glaciomarine sedimentation interpreted from seismic surveys of fiords on Baffin Island, NWT. *Arctic* 38, 271–280.
- Girardclos, S., Schmidt, O.T., Sturm, M., Ariztegui, D., Pugin, A., Anselmetti, F.S., 2007. The 1996 AD delta collapse and large turbidite in Lake Brienz. *Mar. Geol.* 241, 137–154. <https://doi.org/10.1016/j.margeo.2007.03.011>.
- Graham, A.G.C., Hogan, K.A., 2016. Crescentic scour on palaeo-ice stream beds. *Geol. Soc. Lond. Mem.* 46, 221–222.
- Graham, A.G.C., Larter, R.D., Gohl, K., Hillenbrand, C.D., Smith, J.A., Kuhn, G., 2009. Bedform signature of a West Antarctic palaeo-ice stream reveals a multi-temporal record of flow and substrate control. *Quat. Sci. Rev.* 28, 2774–2793. <https://doi.org/10.1016/j.quascirev.2009.07.003>.
- Gudmundsson, G.H., Krug, J., Durand, G., Favier, L., Gagliardini, O., 2012. The stability of grounding lines on retrograde slopes. *Cryosphere* 6, 1497–1505. <https://doi.org/10.5194/tc-6-1497-2012>.
- Halchuk, S., 2009. Seismic Hazard Earthquake Epicentre File (SHEEF) Used in the Fourth Generation Seismic Hazard Maps of Canada. Geological Survey of Canada <https://doi.org/10.4095/261333> (Open File 6208, 2009, 16 pages (1 sheet); 1 CD-ROM).
- Hasegawa, H.S., Adams, J., 1990. Reanalysis of the 1963 Baffin Island earthquake (Ms 6.2) and its seismotectonic environment. *Seismol. Res. Lett.* 61, 181–192.
- Heroy, D.C., Anderson, J.B., 2005. Ice-sheet extent of the Antarctic Peninsula region during the Last Glacial Maximum (LGM) – insights from glacial geomorphology. *Bull. Geol. Soc. Am.* 117, 1497–1512. <https://doi.org/10.1130/B25694.1>.
- Hjelstuen, B.O., Kjennbakken, H., Bleikli, V., Ersland, R.A., Kviliaug, S., Euler, C., Alvheim, S., 2013. Fiord stratigraphy and processes – evidence from the NE Atlantic Fensfjorden system. *J. Quat. Sci.* 28, 421–432. <https://doi.org/10.1002/jqs.2636>.
- Hodgson, D.A., Graham, A.G.C.C., Griffiths, H.J., Roberts, S.J., Ó Cofaigh, C., Bentley, M.J., Evans, D.J.A.A., 2014. Glacial history of sub-Antarctic South Georgia based on the submarine geomorphology of its fjords. *Quat. Sci. Rev.* 89, 129–147. <https://doi.org/10.1016/j.quascirev.2013.12.005>.
- Holtedahl, H., 1967. Notes on the formation of fiords and fiord-valleys. *Geogr. Ann. Ser. A Phys. Geogr.* 49 (2–4), 188–203.
- Howe, J.A., Austin, W.E.N., Forwick, M., Paetzl, M., Harland, R., Cage, A.G., 2010. Fiord systems and archives: a review. *Geol. Soc. Lond. Spec. Publ.* 344, 5–15. <https://doi.org/10.1144/SP344.2>.
- Jackson, G.D., Berman, R.G., 2000. Precambrian metamorphic and tectonic evolution of Northern Baffin Island, Nunavut, Canada. *Can. Mineral.* 38, 399–421. <https://doi.org/10.2113/gscannmin.38.2399>.
- Jakobsson, M., Mayer, L., Coakley, B., Dowdeswell, J.A., Forbes, S., Fridman, B., Hodnesdal, H., Noormets, R., Pedersen, R., Rebese, M., Schenke, H.W., Zarayskaya, Y., Accettella, D., Armstrong, A., Anderson, R.M., Bienhoff, P., Camerlenghi, A., Church, I., Edwards, M., Gardner, J.V., Hall, J.K., Hell, B., Hestvik, O., Kristoffersen, Y., Marcusen, C., Mohammad, R., Mosher, D., Nghiem, S.V., Pedrosa, M.T., Travaglini, P.G., Weatherall, P., 2012. The International Bathymetric Chart of the Arctic Ocean (IBCAO) version 3.0. *Geophys. Res. Lett.* 39. <https://doi.org/10.1029/2012GL052219>.
- Jakobsson, M., Greenwood, S.L., Hell, B., Ó Íáos, H., 2016. Drumlins in the Gulf of Bothnia. *Geol. Soc. Lond. Mem.* 46, 197–198.
- Jamieson, S.S.R., Vieli, A., Livingstone, S.J., Ó Cofaigh, C., Stokes, C., Hillenbrand, C.-D., Dowdeswell, J.A., 2012. Ice-stream stability on a reverse bed slope. *Nat. Geosci.* 5, 799–802. <https://doi.org/10.1038/NGEO1600>.
- Jamieson, S.S.R., Vieli, A., Ó Cofaigh, C., Stokes, C.R., Livingstone, S.J., Hillenbrand, C.D., 2014. Understanding controls on rapid ice-stream retreat during the last deglaciation of Marguerite Bay, Antarctica, using a numerical model. *J. Geophys. Res. Earth Surf.* 119, 247–263. <https://doi.org/10.1020/2013JF002934>.
- Jezek, K., Wu, X., Gogineni, P., Rodríguez, E., Freeman, A., Rodriguez-Morales, F., Clark, C.D., 2011. Radar images of the bed of the Greenland Ice Sheet. *Geophys. Res. Lett.* 38. <https://doi.org/10.1029/2010GL045519>.
- Joughin, I., Alley, R.B., 2011. Stability of the West Antarctic ice sheet in a warming world. *Nat. Geosci.* <https://doi.org/10.1038/ngeo1194>.
- Joughin, I., Alley, R.B., Holland, D.M., 2012. Ice-sheet response to oceanic forcing. *Science* 338, 1172–1176. <https://doi.org/10.1126/science.1226481>.
- King, E.C., Woodward, J., Smith, A.M., 2007. Seismic and radar observations of subglacial bed forms beneath the onset zone of Rutford Ice Stream, Antarctica. *J. Glaciol.* 53, 665–672. <https://doi.org/10.3189/002214307784409216>.
- King, E.C., Hindmarsh, R.C.A., Stokes, C.R., 2009. Formation of mega-scale glacial lineations observed beneath a West Antarctic ice stream. *Nat. Geosci.* 2, 585–588. <https://doi.org/10.1038/ngeo581>.
- Krabbendam, M., 2016. Basal sliding of temperate basal ice on a rough, hard bed: pressure melting, creep mechanisms and implications for ice streaming. *Cryosphere Discuss.* 1–27 <https://doi.org/10.5194/tc-2016-52>.
- Krabbendam, M., Eyles, N., Putkinen, N., Bradwell, T., Arbelaez-Moreno, L., 2016. Streamlined hard beds formed by palaeo-ice streams: a review. *Sediment. Geol.* 338, 24–50. <https://doi.org/10.1016/j.sedgeo.2015.12.007>.
- Lajeunesse, P., 2016. Late Wisconsinan grounding-zone wedges, northwestern Gulf of St Lawrence, eastern Canada. *Geol. Soc. Lond. Mem.* 46, 227–228. <https://doi.org/10.1144/M46.91>.
- Lajeunesse, P., Dietrich, P., Ghienne, J.F., 2018. Late Wisconsinan grounding zones of the Laurentide Ice Sheet margin off the Québec North Shore (NW Gulf of St Lawrence). *Geol. Soc. Lond. Spec. Publ.* 475, SP475–10.

- Lindén, M., Möller, P., 2005. Marginal formation of De Geer moraines and their implications to the dynamics of grounding-line recession. *J. Quat. Sci.* 20, 113–133.
- Livingstone, S.J., Ó Cofaigh, C., Stokes, C.R., Hillenbrand, C.D., Vieli, A., Jamieson, S.S.R., 2012. Antarctic palaeo-ice streams. *Earth Sci. Rev.* 111, 90–128. <https://doi.org/10.1016/j.earscirev.2011.10.003>.
- Livingstone, S.J., Ó Cofaigh, C., Stokes, C.R., Hillenbrand, C.D., Vieli, A., Jamieson, S.S.R., 2013. Glacial geomorphology of Marguerite Bay Palaeo-Ice stream, western Antarctic Peninsula. *J. Maps* <https://doi.org/10.1080/17445647.2013.829411> (9419254120, 558–57 240).
- Lowe, A.L., Anderson, J.B., 2003. Evidence for abundant subglacial meltwater beneath the paleo-ice sheet in Pine Island Bay, Antarctica. *J. Glaciol.* 49, 125–138. <https://doi.org/10.3189/172756503781830971>.
- MacLean, B., Blasco, S., Bennett, R., Clarke, J.E.H., Patton, E., 2016a. Moat features, Amundsen Gulf, Canadian Arctic Archipelago. *Geol. Soc. Lond. Mem.* 46, 51–52.
- MacLean, B., Blasco, S., Bennett, R., Clarke, J.E.H., Patton, E., 2016b. Mega-scale glacial linations, Peel Sound, Canadian Arctic Archipelago. *Geol. Soc. Lond. Mem.* 46, 47–48.
- MacLean, B., Blasco, S., Bennett, R., Lakeman, T., Pieńkowski, A.J., Furze, M.F.A., Clarke, J.E.H., Patton, E., 2017. Seafloor features delineate Late Wisconsinan ice stream configurations in eastern Parry Channel, Canadian Arctic Archipelago. *Quat. Sci. Rev.* 160, 67–84. <https://doi.org/10.1016/j.quascirev.2017.02.001>.
- Margold, M., Stokes, C.R., Clark, C.D., 2015a. Ice streams in the Laurentide Ice Sheet: identification, characteristics and comparison to modern ice sheets. *Earth Sci. Rev.* 143, 117–146. <https://doi.org/10.1016/j.earscirev.2015.01.011>.
- Margold, M., Stokes, C.R., Clark, C.D., Kleman, J., 2015b. Ice streams in the Laurentide Ice Sheet: new mapping inventory. *J. Maps* 11, 380–395. <https://doi.org/10.1080/17445647.2014.912036>.
- Meier, M.F., Post, A., 1987. Fast tidewater glaciers. *J. Geophys. Res.* 92, 9051. <https://doi.org/10.1029/JB092iB09p09051>.
- Menzies, J., 1979. A review of the literature on the formation and location of drumlins. *Earth Sci. Rev.* 14 (4), 315–359.
- Mercer, J.H., 1978. West Antarctic ice sheet and CO₂ greenhouse effect: a threat of disaster. *Nature* 271, 321–325. <https://doi.org/10.1038/271321a0>.
- Miller, G.H., Wolfe, A.P., Steig, E.J., Sauer, P.E., Kaplan, M.R., Briner, J.P., 2002. The goldilocks dilemma: big ice, little ice, or “just-right” ice in the eastern Canadian arctic. *Quat. Sci. Rev.* 21, 33–48. [https://doi.org/10.1016/S0277-3791\(01\)00085-3](https://doi.org/10.1016/S0277-3791(01)00085-3).
- Miller, G.H., Wolfe, A.P., Briner, J.P., Sauer, P.E., Nesje, A., 2005. Holocene glaciation and climate evolution of Baffin Island, Arctic Canada. *Quat. Sci. Rev.* 24, 1703–1721. <https://doi.org/10.1016/j.quascirev.2004.06.021>.
- Morlighem, M., Williams, C.N., Rignot, E., An, L., Bamber, J.L., Catania, G., Dowdeswell, J.A., Dorschel, B., Fenty, I., Hogan, K., Howat, I., Hubbard, A., Jakobsson, M., Jordan, T.M., Kjeldsen, K.K., Millan, R., Mayer, L., Mouginot, J., Palmer, S., Rysgaard, S., Seroussi, H., Slabon, P., Straneo, F., Weinrebe, W., Wood, M., Zinglersen, B., Arndt, J.E., Bamber, J.L., Chauché, N., 2017. BedMachine v3: complete bed topography and ocean bathymetry mapping of Greenland from multi-beam echo sounding combined with mass conservation. *Geophys. Res. Lett.* <https://doi.org/10.1002/2017GL074954>.
- Nagler, T., Rott, H., Hetzenecker, M., Wuite, J., Potin, P., 2015. The Sentinel-1 mission: new opportunities for ice sheet observations. *Remote Sens.* 7, 9371–9389. <https://doi.org/10.3390/rs70709371>.
- Nemec, W., 2009. Aspects of sediment movement on steep delta slopes. Coarse-grained Deltas, pp. 29–73 <https://doi.org/10.1002/9781444303858.ch3>.
- Nick, F.M., Van Der Veen, C.J., Vieli, A., Benn, D.I., 2010. A physically based calving model applied to marine outlet glaciers and implications for the glacier dynamics. *J. Glaciol.* 56, 781–794. <https://doi.org/10.3189/002214310794457344>.
- Nitsche, F.O., Gohl, K., Larter, R.D., Hillenbrand, C.D., Kuhn, G., Smith, J.A., Jacobs, S., Anderson, J.B., Jakobsson, M., 2013. Paleo ice flow and subglacial meltwater dynamics in Pine Island Bay, West Antarctica. *Cryosphere* 7, 249–262. <https://doi.org/10.5194/tc-7-249-2013>.
- Ó Cofaigh, C., Dowdeswell, J.A., Allen, C.S., Hiemstra, J.F., Pudsey, C.J., Evans, J., Evans, D.J.A., 2005. Flow dynamics and till genesis associated with a marine-based Antarctic palaeo-ice stream. *Quat. Sci. Rev.* <https://doi.org/10.1016/j.quascirev.2004.10.006>.
- Osterman, L.E., Nelson, A.R., 1989. Latest Quaternary and Holocene paleoceanography of the eastern Baffin Island continental shelf, Canada: benthic foraminiferal evidence. *Can. J. Earth Sci.* 26, 2236–2248. <https://doi.org/10.1139/e89-190>.
- Ottesen, D., Dowdeswell, J.A., 2009. An inter-ice-stream glaciated margin: submarine landforms and a geomorphic model based on marine-geophysical data from Svalbard. *Bull. Geol. Soc. Am.* 121, 1647–1665. <https://doi.org/10.1130/B26467.1>.
- Ottesen, D., Dowdeswell, J.A., Benn, D.I., Kristensen, L., Christiansen, H.H., Christensen, O., Hansen, L., Lebesbye, E., Forwick, M., Vorren, T.O., 2008. Submarine landforms characteristic of glacier surges in two Spitsbergen fjords. *Quat. Sci. Rev.* 27, 1583–1599. <https://doi.org/10.1016/j.quascirev.2008.05.007>.
- Ottesen, D., Dowdeswell, J.A., Bellec, V.K., Bjarnadóttir, L.R., 2017. The geomorphic imprint of glacier surges into open-marine waters: examples from eastern Svalbard. *Mar. Geol.* 392, 1–29. <https://doi.org/10.1016/j.margeo.2017.08.007>.
- Paull, C.K., Ussler III, W., Caress, D.W., Lundsten, E., Covault, J.A., Maier, K.L., Xu, J., Augenstein, S., 2010. Origins of large crescent-shaped bedforms within the axial channel of Monterey Canyon, offshore California. *Geosphere* 6, 755–774. <https://doi.org/10.1130/GES00527.1>.
- Paull, C.K., Caress III, D.W., WU, Lundsten, E., Meiner-Johnson, M., 2011. High-resolution bathymetry of the axial channels within Monterey and Soquel submarine canyons, offshore central California. *Geosphere* 7, 1077–1101. <https://doi.org/10.1130/GES00636.1>.
- Peltz, M.S., Warren, C.R., 1991. Relationship between tidewater glacier calving velocity and water depth at the calving front. *Ann. Glaciol.* 15, 115–118.
- Powell, R.D., 2003. Subaqueous landsystems: fjords. *Glacial Landsystems*, pp. 313–347.
- Praeg, D., Maclean, B., Sonnichsen, G., 2007. Quaternary geology of the Northeast Baffin Island Continental Shelf, Cape Aston to Buchan Gulf (70° to 72°N). *Geological Survey of Canada Open File Report*.
- Rebesco, M., Liu, Y., Camerlenghi, A., Winsborrow, M., Laberg, J.S., Caburlotto, A., Diviacco, P., Accettella, D., Sauli, C., Wardell, N., Tomini, I., 2011. Deglaciation of the western margin of the Barents Sea Ice Sheet - a swath bathymetric and sub-bottom seismic study from the Kveithola Trough. *Mar. Geol.* 279, 141–147. <https://doi.org/10.1016/j.margeo.2010.10.018>.
- Reinardy, B.T.I., Larter, R.D., Hillenbrand, C.D., Murray, T., Hiemstra, J.F., Booth, A.D., 2011. Streaming flow of an Antarctic Peninsula palaeo-ice stream, both by basal sliding and deformation of substrate. *J. Glaciol.* 57, 596–608. <https://doi.org/10.3189/002214311797409758>.
- Rignot, E., Velicogna, I., Van Den Broeke, M.R., Monaghan, A., Lenaerts, J., 2011. Acceleration of the contribution of the Greenland and Antarctic ice sheets to sea level rise. *Geophys. Res. Lett.* 38. <https://doi.org/10.1029/2011GL046583>.
- Schoof, C., 2007. Ice sheet grounding line dynamics: Steady states, stability, and hysteresis. *J. Geophys. Res. Earth Surf.* 112. <https://doi.org/10.1029/2006JF000664>.
- Shepherd, A., Ivins, E.R., AG, Barletta, V.R., Bentley, M.J., Bettadpur, S., Briggs, K.H., Bromwich, D.H., Forsberg, R., Galin, N., Horwath, M., Jacobs, S., Jouhijn, I., King, M.A., Lenaerts, J.T.M., Li, J., Ligtenberg, S.R.M., Luckman, A., Luthcke, S.B., McMillan, M., Meister, R., Milne, G., Mouginot, J., Muir, A., Nicolas, J.P., Paden, J., Payne, A.J., Pritchard, H., Rignot, E., Rott, H., Sorensen, L.S., Scambos, T.A., Scheuchl, B., Schrama, E.J.O., Smith, B., Sundal, A.V., van Angelen, J.H., van de Berg, W.J., van den Broeke, M.R., Vaughan, D.G., Velicogna, I., Wahr, J., Whitehouse, P.L., Wingham, D.J., Yi, D., Young, D., Zwally, H.J., 2012. A reconciled estimate of ice-sheet mass balance. *Science* 338, 1183–1189. <https://doi.org/10.1126/science.1228102>.
- Smith, J.A., Hillenbrand, C.D., Larter, R.D., Graham, A.G.C., Kuhn, G., 2009. The sediment infill of subglacial meltwater channels on the West Antarctic continental shelf. *Quat. Res.* 71, 190–200. <https://doi.org/10.1016/j.yqres.2008.11.005>.
- Stein, S., Sleep, N.H., Geller, R.J., Wang, S., Kroeger, G.C., 1979. Earthquakes along the passive margin of eastern Canada. *Geophys. Res. Lett.* 6, 537–540.
- Stokes, C.R., Clark, C.D., 2002. Are long subglacial bedforms indicative of fast ice flow? *Boreas* 31, 239–249. <https://doi.org/10.1111/j.1502-3885.2002.tb01070.x>.
- Stokes, C.R., Clark, C.D., Lian, O.B., Tulaczyk, S., 2007. Ice stream sticky spots: a review of their identification and influence beneath contemporary and palaeo-ice streams. *Earth Sci. Rev.* <https://doi.org/10.1016/j.earscirev.2007.01.002>.
- Stokes, C.R., Spagnolo, M., Clark, C.D., 2011. The composition and internal structure of drumlins: complexity, commonality, and implications for a unifying theory of their formation. *Earth Sci. Rev.* 107 (3–4), 398–422.
- Stravers, J.A., Syvitski, J.P.M., 1991. Land-sea correlations and evolution of the Cambridge Fiord marine basin during the last deglaciation of Northern Baffin island. *Quat. Res.* 35, 72–90. [https://doi.org/10.1016/0033-5894\(91\)90096-N](https://doi.org/10.1016/0033-5894(91)90096-N).
- Syvitski, J.P.M., Shaw, J., 1995. Chapter 5 sedimentology and geomorphology of fjords. *Dev. Sedimentol.* 53, 113–178. [https://doi.org/10.1016/S0070-4571\(05\)80025-1](https://doi.org/10.1016/S0070-4571(05)80025-1).
- Syvitski, J., Burrell, D., Skei, J., 1987. Fjords: Processes and Products. Springer Verlag <https://doi.org/10.1017/CBO9781107415324.004>.
- Todd, B.J., Valentine, P.C., Longva, O., Shaw, J., 2007. Glacial landforms on German Bank, Scotian Shelf: evidence for Late Wisconsinan ice-sheet dynamics and implications for the formation of De Geer moraines. *Boreas* 36, 148–169. <https://doi.org/10.1111/j.1502-3885.2007.tb01189.x>.
- van den Broeke, M., Bamber, J., Ettema, J., Rignot, E., Schrama, E., van de Berg, W.J., van Meijgaard, E., Velicogna, I., Wouters, B., 2009. Partitioning recent Greenland mass loss. *Science* 326, 984–986. <https://doi.org/10.1126/science.1178176>.
- Winsborrow, M.C.M., Clark, C.D., Stokes, C.R., 2010. What controls the location of ice streams? *Earth Sci. Rev.* 103, 45–59. <https://doi.org/10.1016/j.earscirev.2010.07.003>.
- Young, N.E., Briner, J.P., Rood, D.H., Finkel, R.C., 2012. Glacier extent during the Younger Dryas and 8.2-ka event on Baffin Island, Arctic Canada. *Science* 337, 1330–1333. <https://doi.org/10.1126/science.1222759>.